LIGO

Review of Accelerometer developments for Gravitational Wave Interferometers

Mechanical noise studies

Seismic signals from GWI seismic isolation systems

Riccardo DeSalvo et al.

20th of September 2007

LIGO-G070640-00-R

LIGO

Motivations for accelerometry

In-Vacuum Accelerometers were developed by Virgo, and later at LIGO for:

- Active Seismic Attenuation
- Inertial damping of rigid body resonances

Motivations for custom accelerometry

- Design accelerometers sensitive exclusively to a single degree of freedom (for feedback)
- Eliminate acoustic and air viscosity noise in vacuum
- Eliminate risk connected with possible leaks from pressurized vessels containing in-air accelerometers
- Better thermal stabilization

LIGO

Waning Motivations

The use of accelerometers for active attenuation was abandoned by Virgo in 1995:

- Because the passive pre-attenuator stage is practically a giant seismometer, with the same limitations of accelerometers
- Because of the principle of equivalence that mixes tilt with horizontal acceleration (but in attenuation one can in part circumvent the problem)
- It is difficult to improve over a 30 mHz Inverted Pendulum platform with accelerometers which are limited by the same material properties that limit the performance of the accelerometers themselves

LIGO

Tilt meters Rekindled Motivations

- Interest rekindled in tiltmeters

- because the **principle of equivalence** is the limiting factor in Inverted Pendula for residual r.m.s.
- The material limitations may still limit the performance

- Thermal Noise
- Hysteresis
- Two faces of the same coin or different limitations?
- Is the r.m.s. noise coming from tilt?

LIGO

- Review of the accelerometer developments

Virgo accelerometers Conceptual design

- Force feedback
- LVDT displacement sensor
- Voice Coil feedback

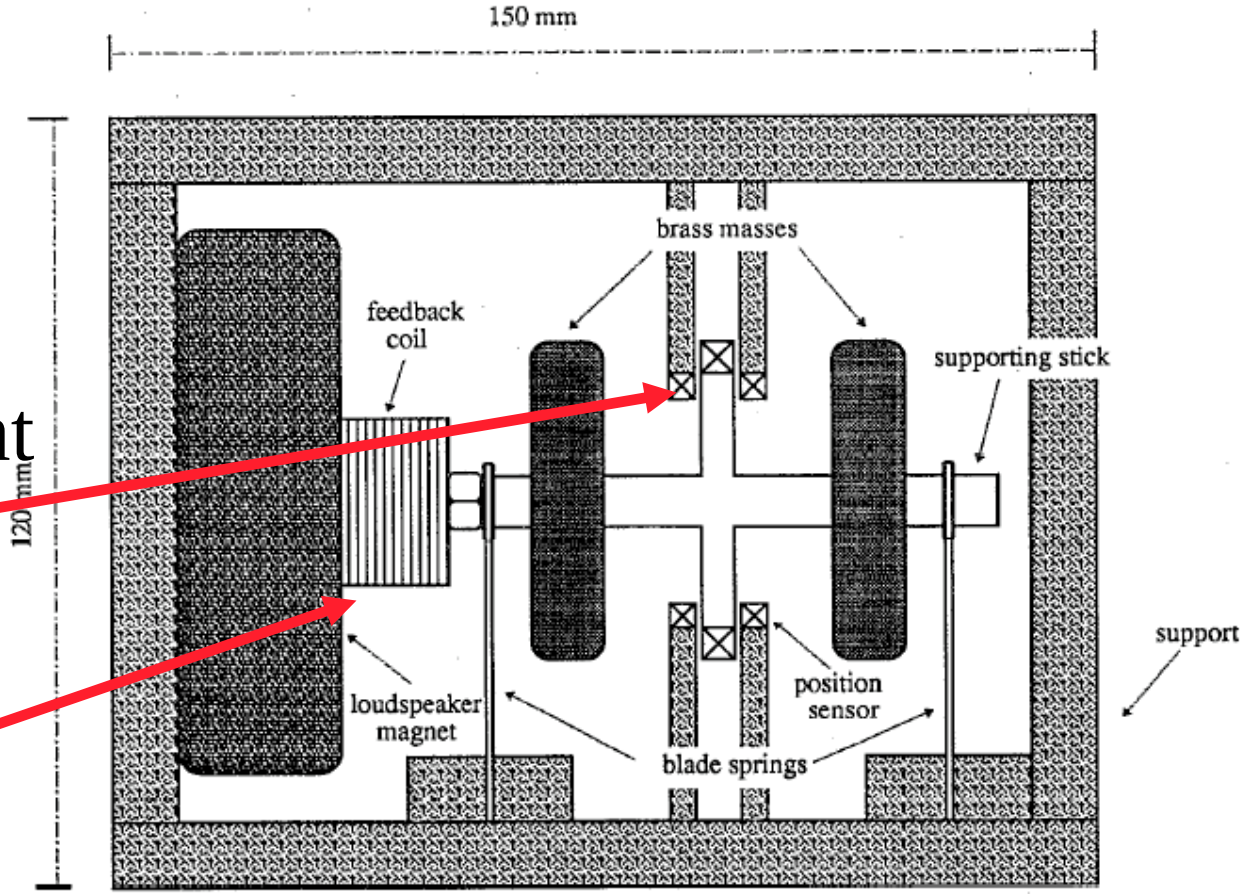

FIG. 2. Drawing of the accelerometer mechanics (side view).

Conceptual design

- Dual flex joints constrain movement in X direction
- IP flex joint configuration used to reduce resonant frequency

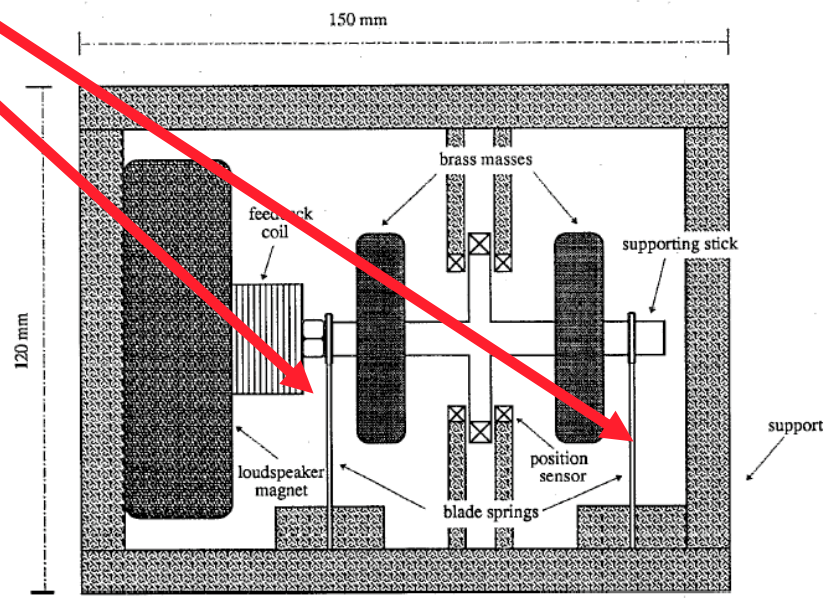

FIG. 2. Drawing of the accelerometer mechanics (side view).

Rev. Sci. Instrum., Vol. 66, No. 3, March 1995

Accelerometer

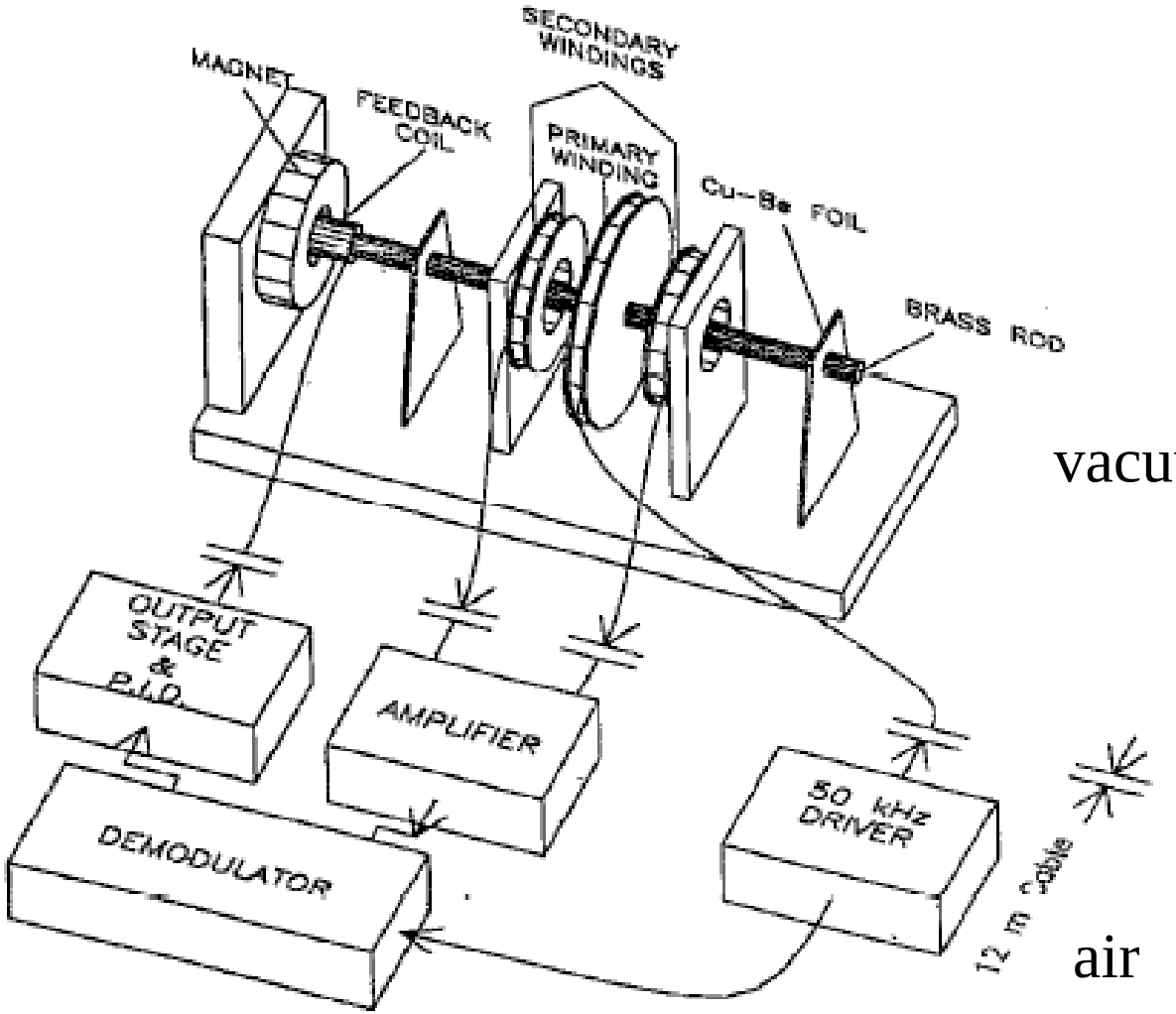

FIG. 1. Schematic drawing of the accelerometer: a block diagram of the control electronics is shown.

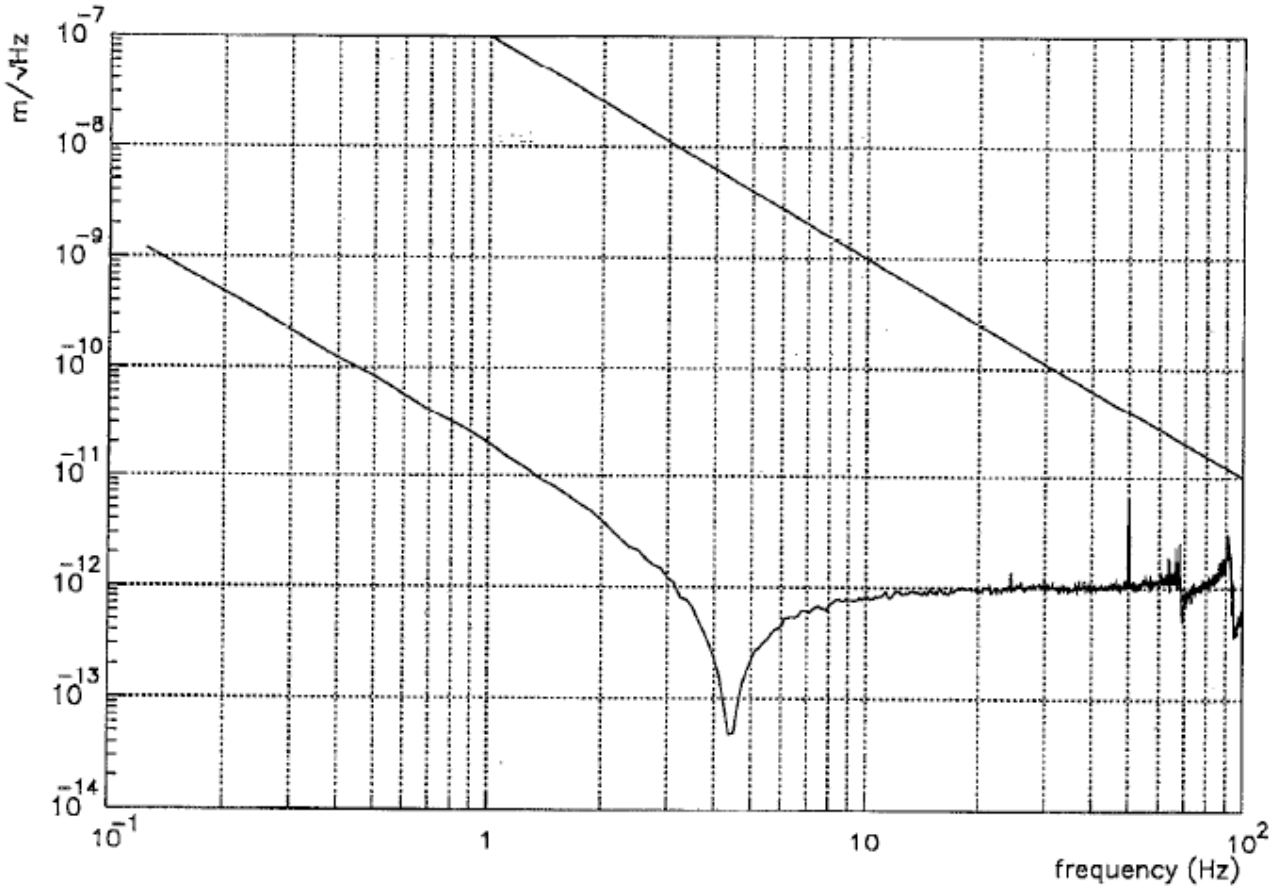

FIG. 5. Displacement spectral sensitivity function (compared with the behavior of a typical spectrum of seism: $x_{\text{seism}}(f) = 10^{-7}/f^2$ m/$\sqrt{\text{Hz}}$).

LIGO

Present Virgo Accelerometers

R. Stanga, F. Paoletti, A.Gennai,

G. Losurdo

LIGO

...Horizontal and vertical...

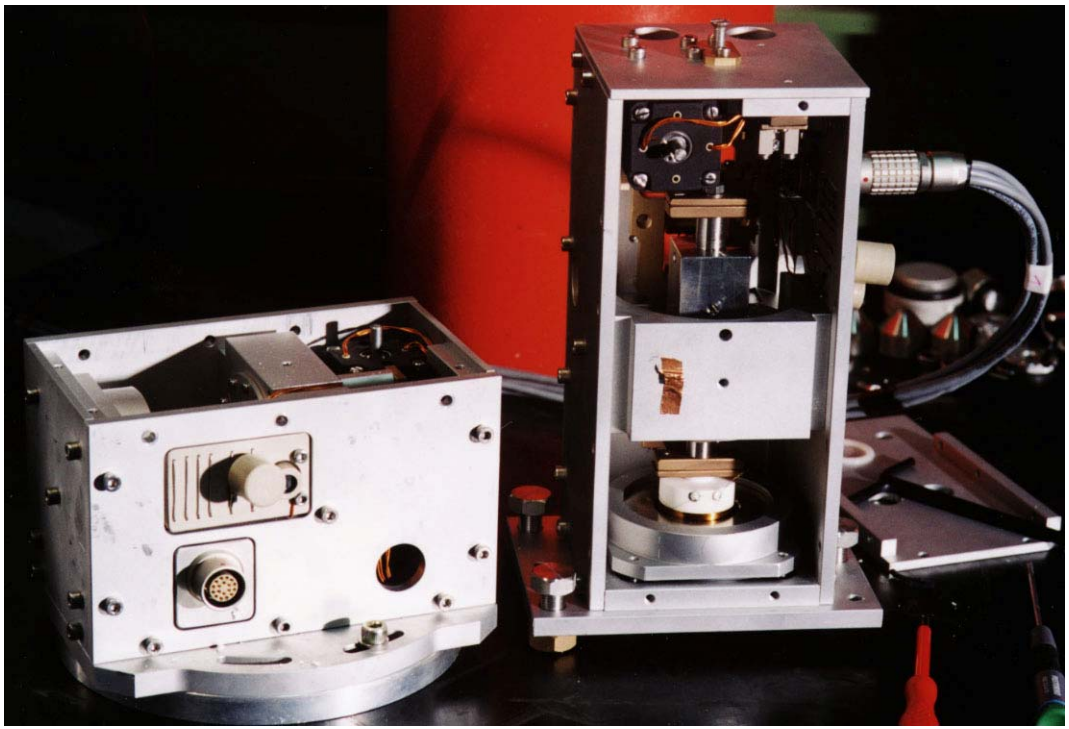

LIGO

Test site, a French ICMB silo

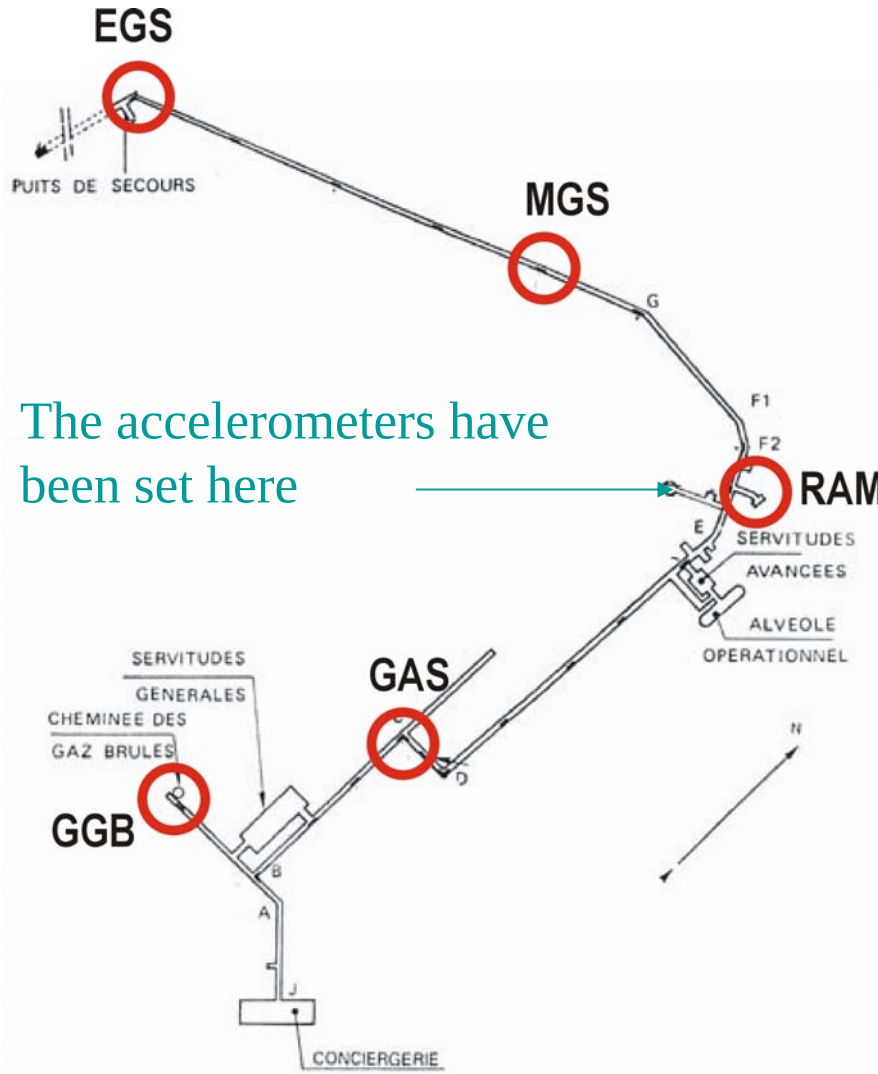

The accelerometers have been set here

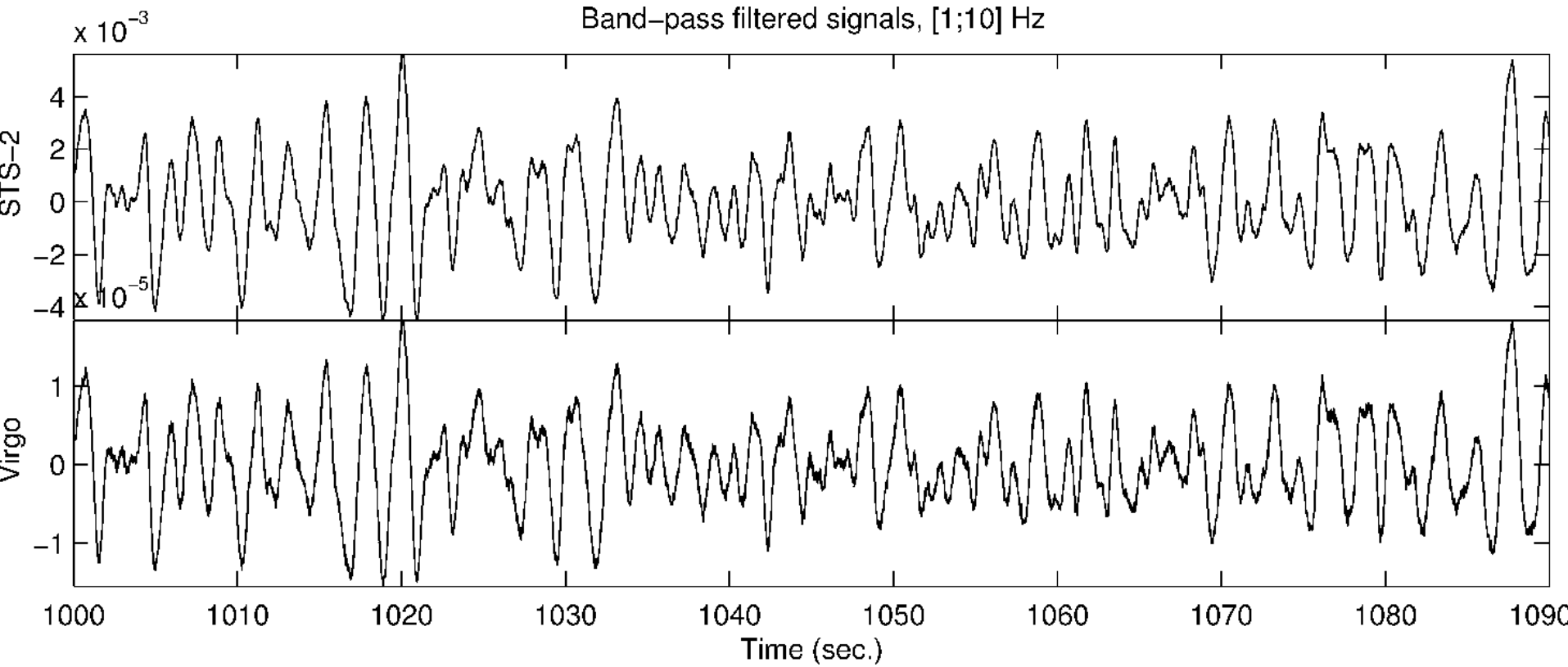

Seism in Japan, 2001 March 24, uncalibrated

Next generation of horizontal accelerometers

- Folded pendulum to lower resonant frequency
- Monolithic construction
- Differential Capacitive sensor
- Surface treatment to minimize material limitations

- Rigidity against the other 5 degrees of freedom

- Alessandro Bertolini at LIGO, and later University of Pisa
- Original folded pendulum Idea from UWA

LIGO Folded Pendulum Mechanical Model

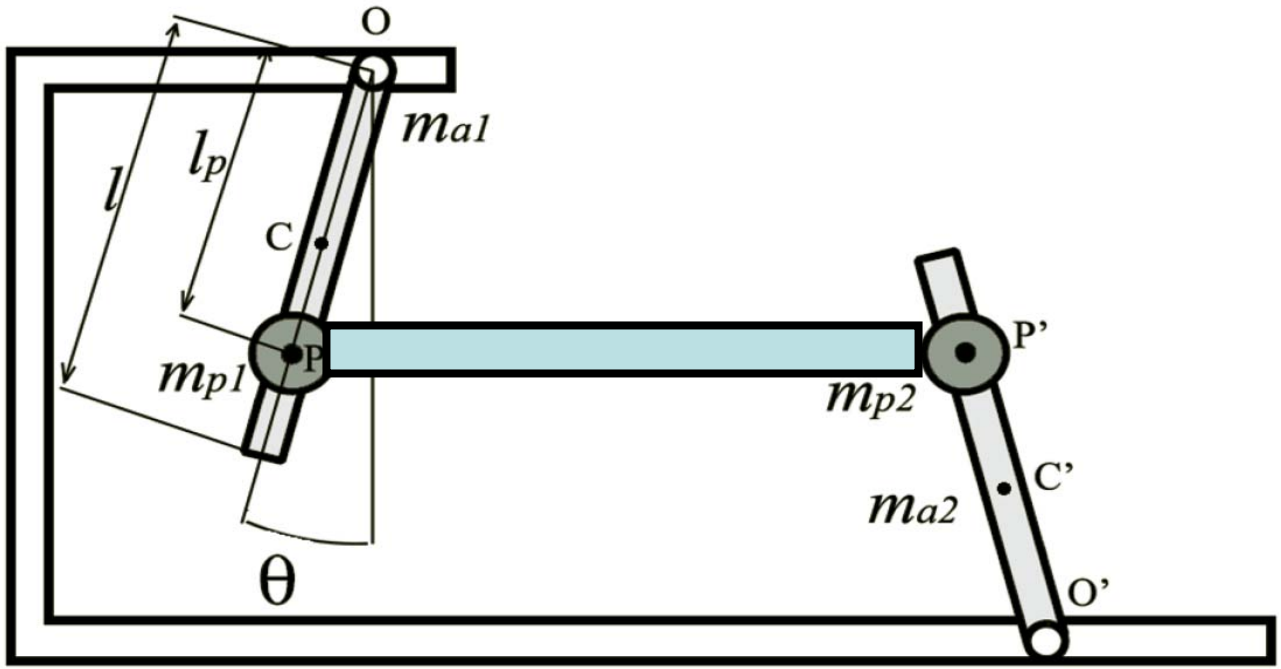

$$\omega_0^2 = \left(\frac{g}{l_p}\right) \cdot \frac{\left(m_{a_1} - m_{a_2}\right)\frac{l}{2l_p} + \left(m_{p_1} - m_{p_2}\right) + \frac{k}{gl_p}}{\left(m_{a_1} + m_{a_2}\right)\frac{l^2}{3l_p} + \left(m_{p_1} + m_{p_2}\right)}$$

LIGO

The mechanics is shaped as a monolithic folded pendulum (Watt linkage) allowing a low resonant frequency (~0.5 Hz) with short pendulum length (~7 cm).

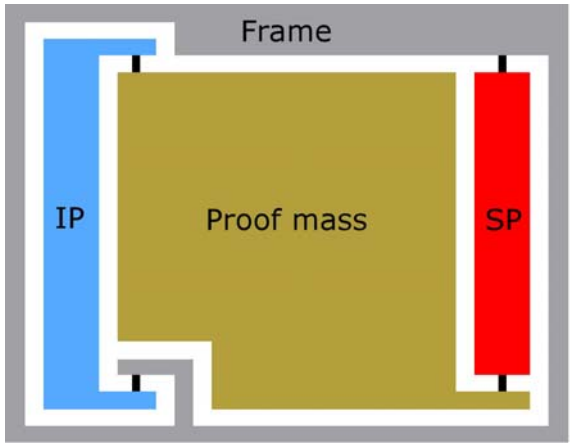

FP principle: balancing between a simple and an inverted pendulum

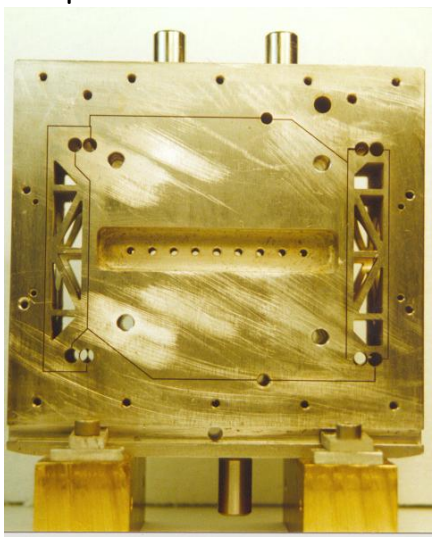

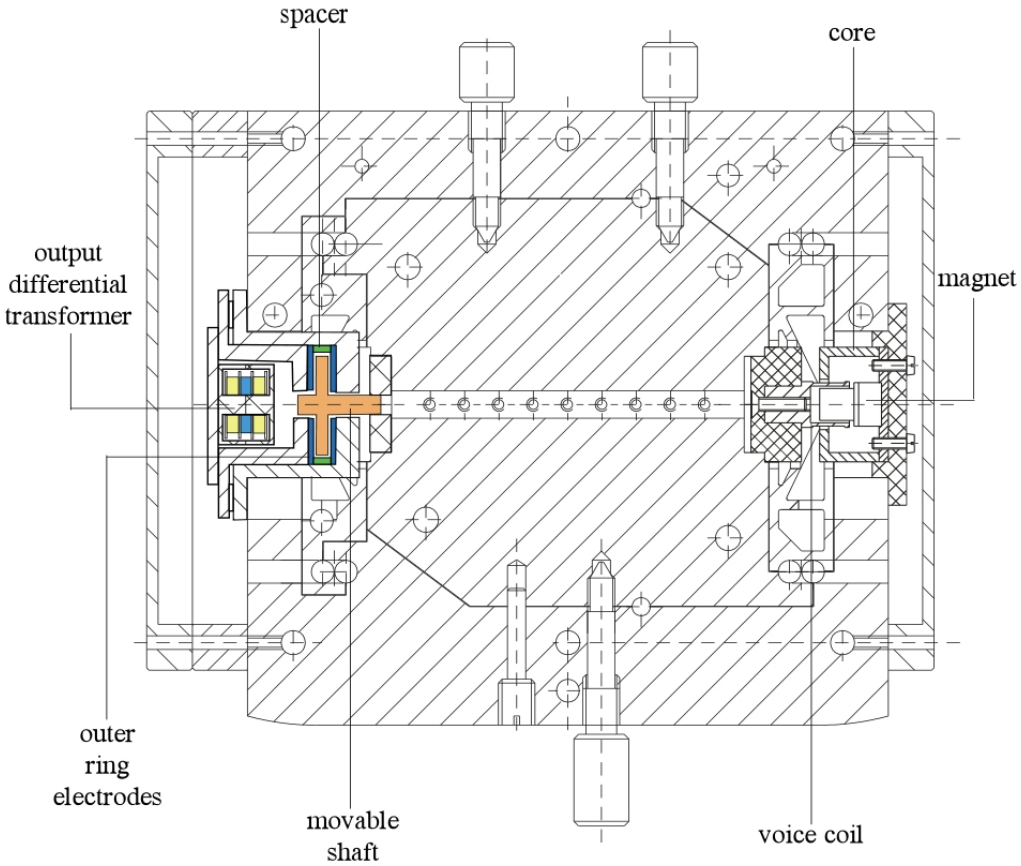

Monolithic FP accelerometer cross section

Multi-DOF active seismic isolation systems need inertial sensors with very low cross-axis sensitivity: rejection factors larger than 80 dB achieved with a monolithic mechanics machined with wire EDM;

the monolithic design allows to eliminate stick-and-slip friction and very high quality factors, Q~3000 @ 0.5 Hz, have been achieved.

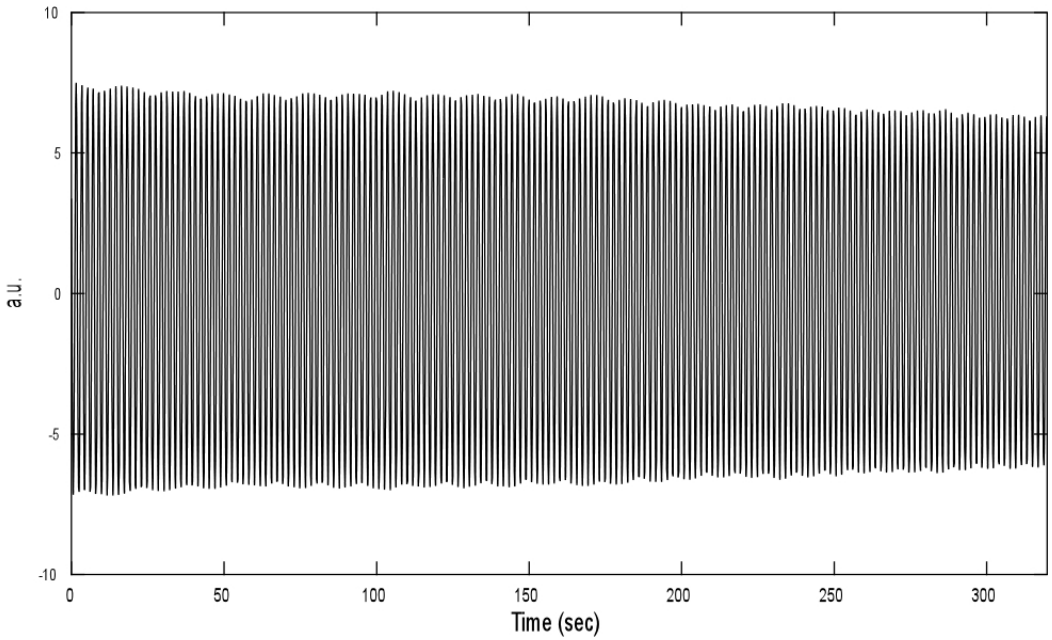

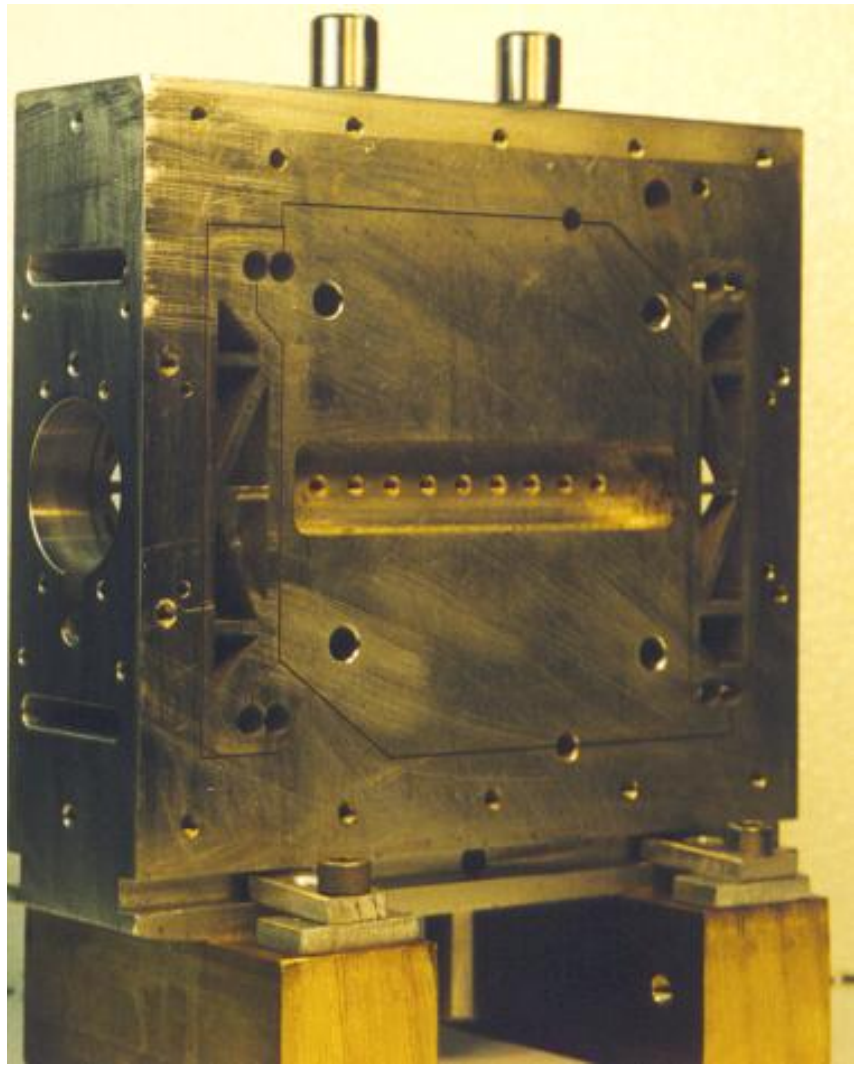

Mechanical resonance decay curve measured in vacuum; the decay time constant is ~ 2300 sec

The accelerometer is equipped with a low noise capacitance sensor driven by a remote signal conditioner; no active components are used on-board. Instrument's performances not compromised by cabling lengths of up to 15 m!

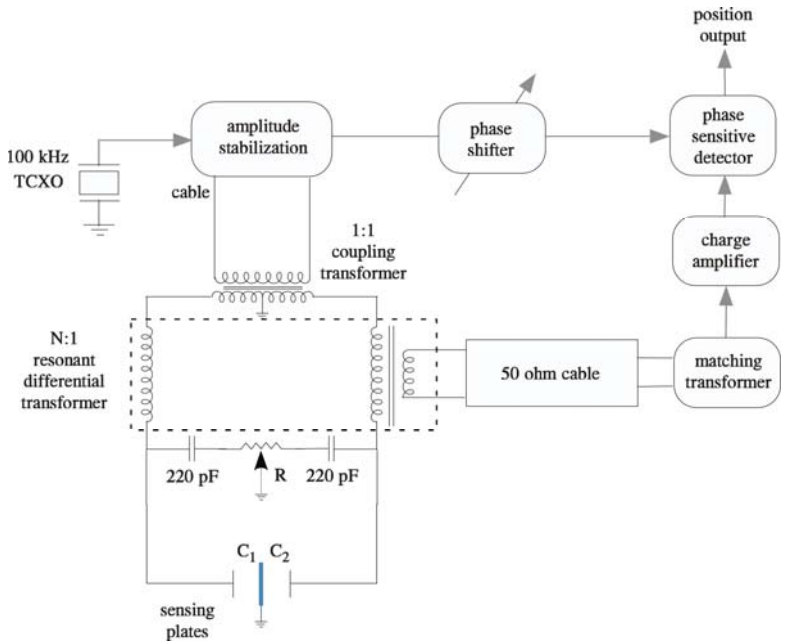

Position sensor electronics block scheme

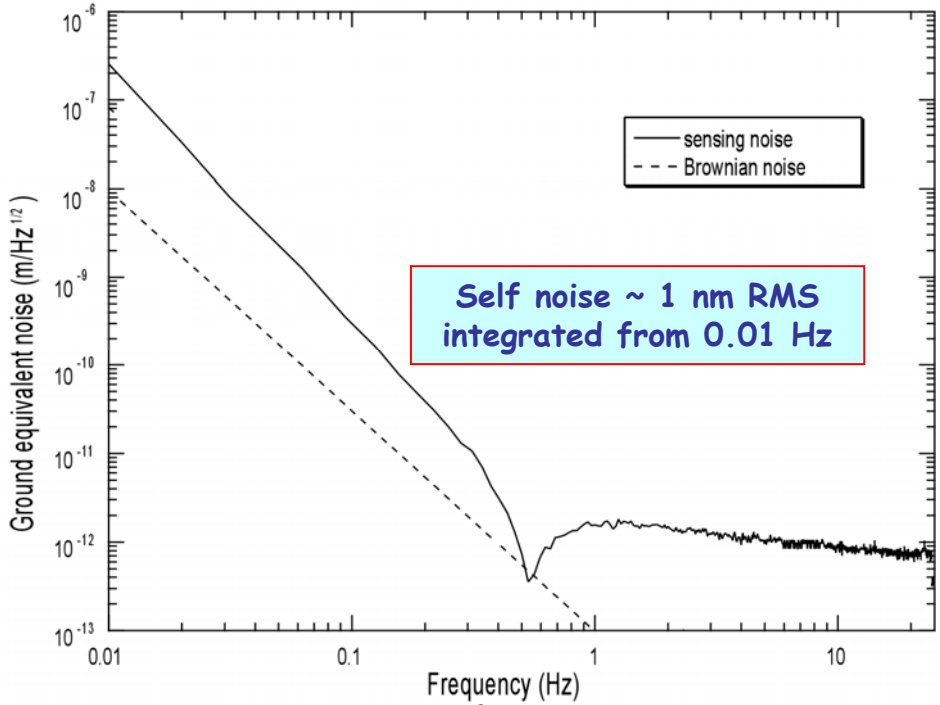

Noise perfomances

A. Bertolini, R. DeSalvo, F. Fidecaro, M. Francesconi, S. Marka, V. Sannibale, D. Simonetti, A. Takamori, H. Tariq, NIM A 564 (2006) 579-586

A. Bertolini, R. DeSalvo, F. Fidecaro, M. Francesconi, S. Marka, V. Sannibale, D. Simonetti, A. Takamori, H. Tariq, NIM A, 556 (2006) 616-623

A. Bertolini, R. DeSalvo, F. Fidecaro, A. Takamori, IEEE TGRS, vol.44 (2006) 273-276

LIGO

FP Continuing development

- The Salerno group

Motivations:

- GW
- Seismology
- Study of Fundamental limitations

LIGO

Mechanical Monolithic Sensors for low frequency seismic noise measurement

F. Acernese [a,b], R. De Rosa [b,c], G. Giordano [b,c], R. Romano [a,c], F. Barone [a,b]

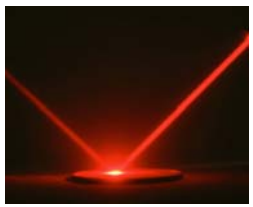

Laboratorio di Fisica Applicata, Dipartimento di Scienze Farmaceutiche, Università degli Studi di Salerno, Italy

[a] Dipartimento di Scienze Farmaceutiche, Università degli Studi di Salerno, Italia

[b] INFN Sezione di Napoli, Napoli, Italia

[c] Dipartimento di Scienze Fisiche, Università degli Studi di Napoli Federico II, Napoli, Italia

LIGO

The prototype

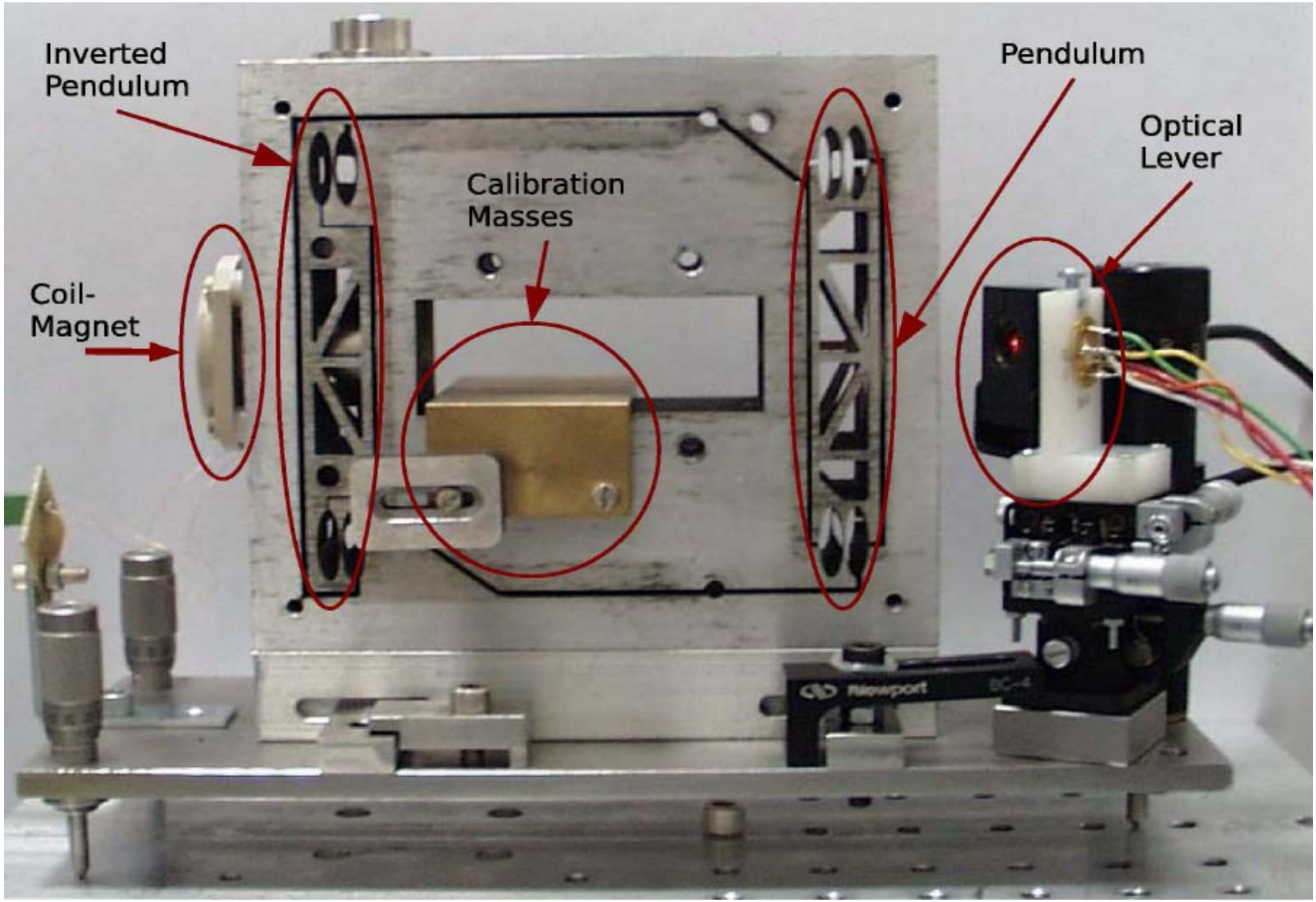

Flex Joints Simulation

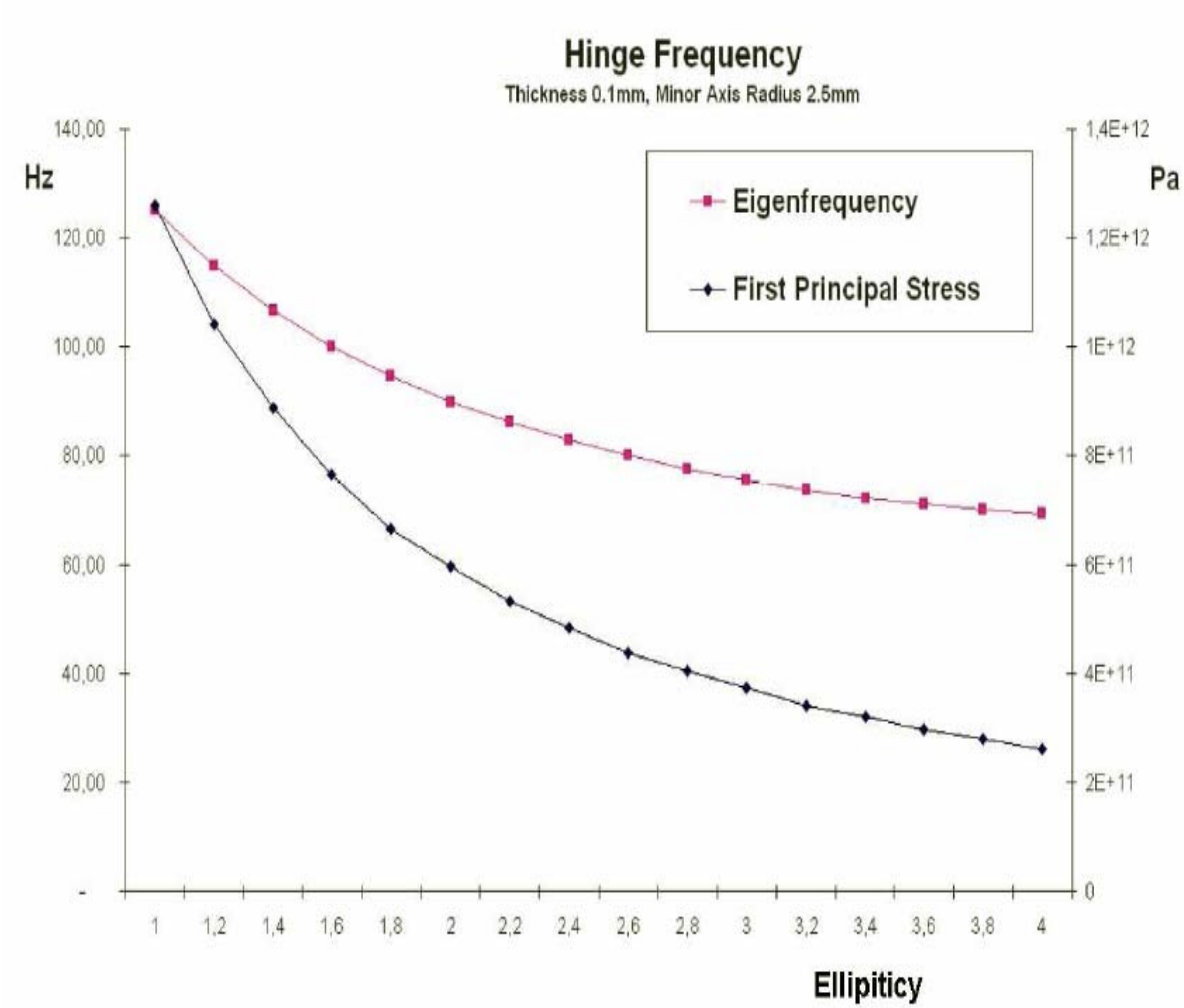

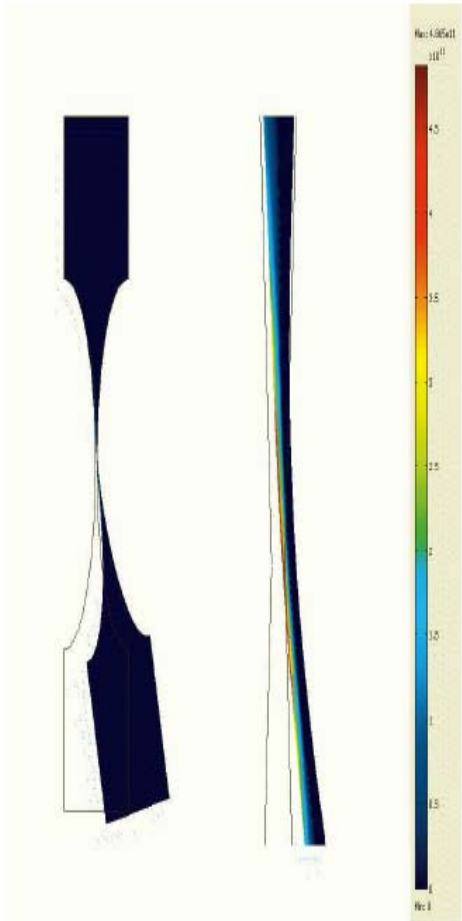

LIGO

Best Results

- Natural Resonance Frequency in open loop configuration (seismometer): 70 mHZ
- Q-Factor: 140

Improved flex joint design:

- Frequency scaled **improvement of Q-factor** by a factor of **2.4** with respect to Bertolini's

- Less fragility

Optical readout configuration

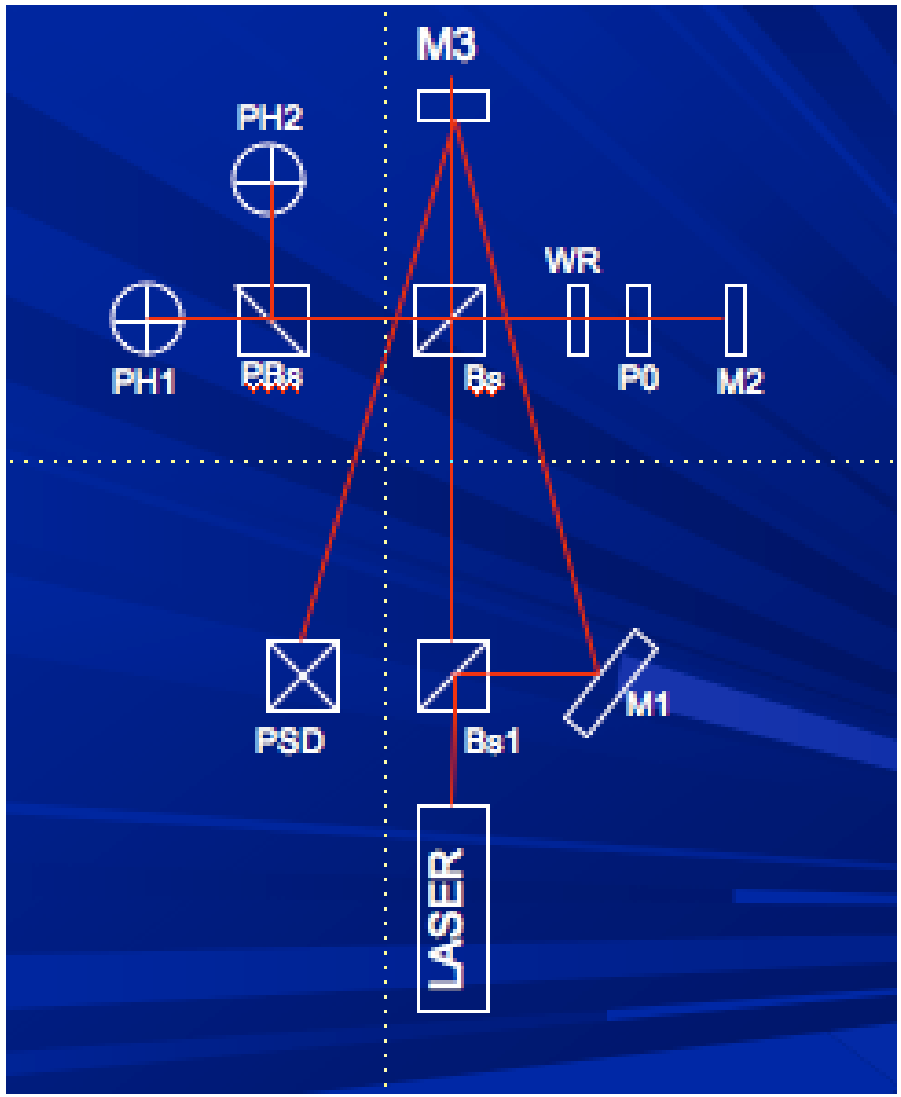

Sensitivity curve in Open Loop configuration

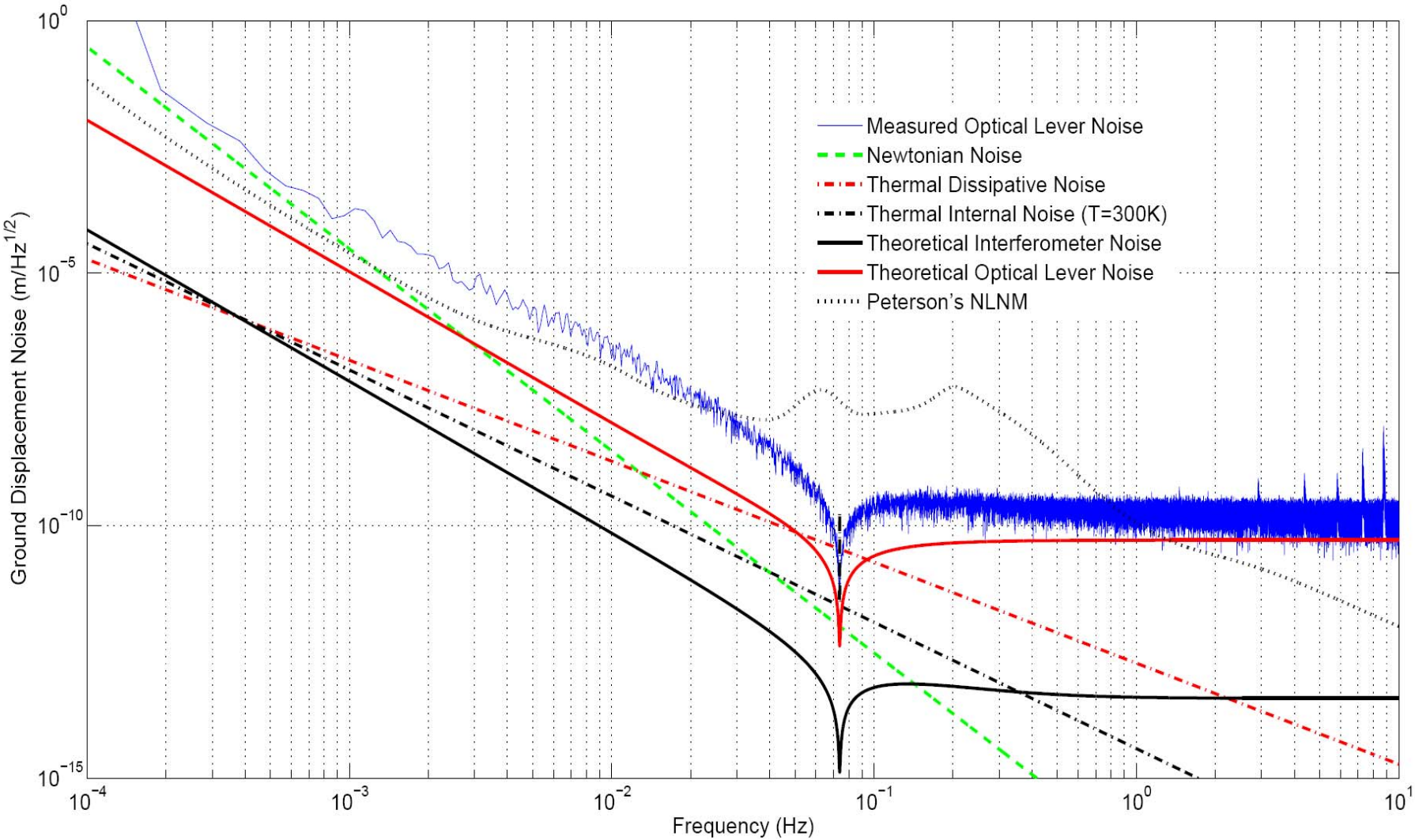

FP tiltmeter developments

- Akiteru Takamori

- Miniaturization
- Fiber readout

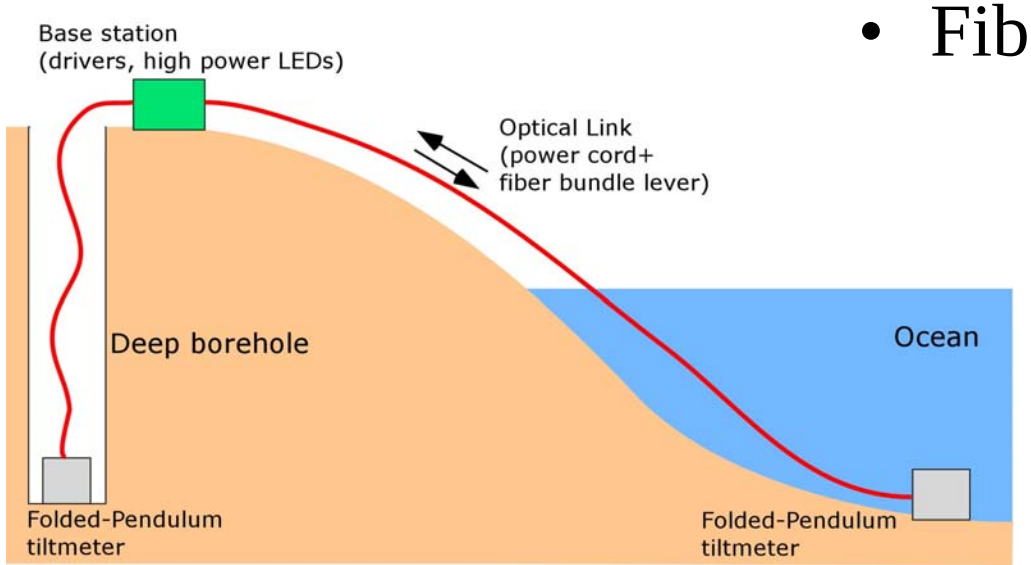

F-P Tiltmeter: Application

- Miniaturized Version for Borehole Obs.
  - Effective Length: ~ 1.0 m
    - Vs. Physical Length: 0.04 m

Compact FP
For Borehole Tiltmeter

FP Accelerometer
Developed for GW Experiment

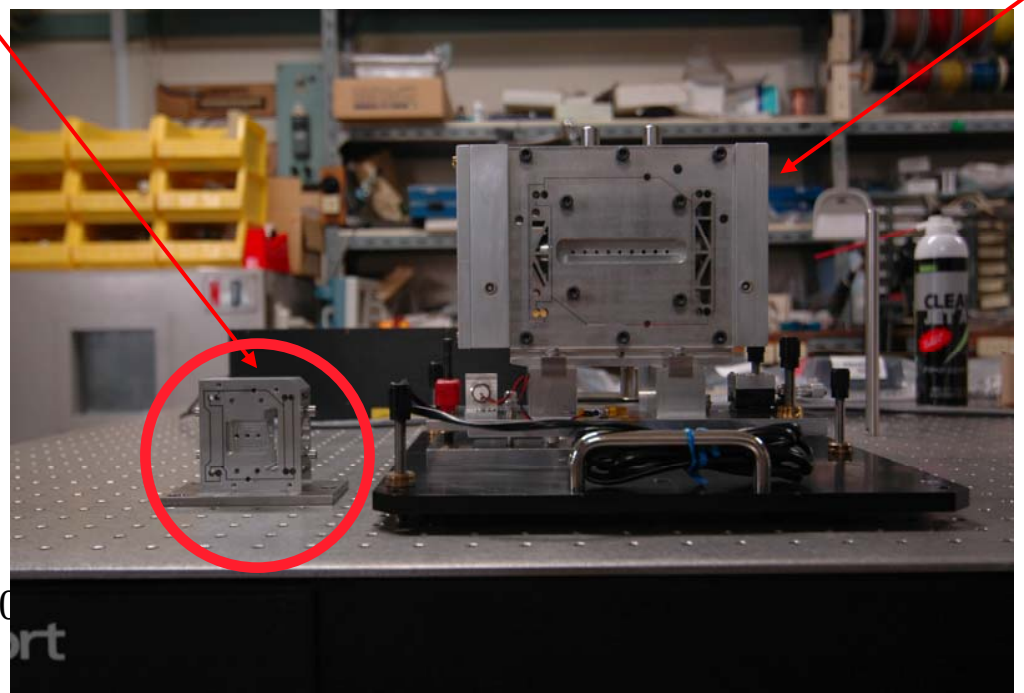

Fiber bundle readout

- Random fiber bundle
- Half illuminated
- Half readout
- Moving surface within ~5 time average fiber spacing
- Longitudinal motion generate widening of all spots and linear increase of transmittance in receiver fibers

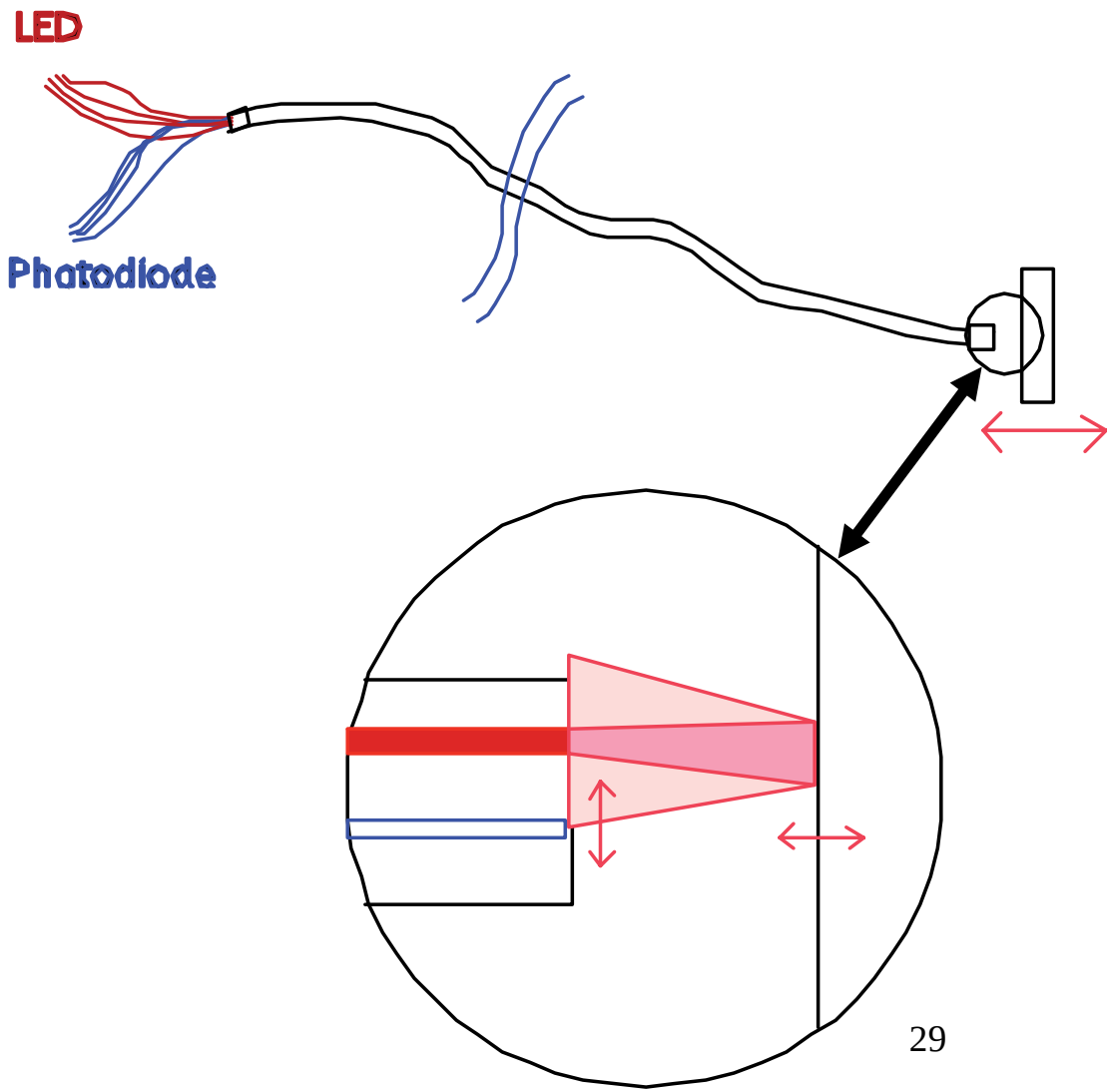

Borehole F-P Tiltmeter

- Prototype Designed to Fit inside Deepsea Boreholes
  - Being Evaluated in Vault
    - Good Agreement with WT Tiltmeter

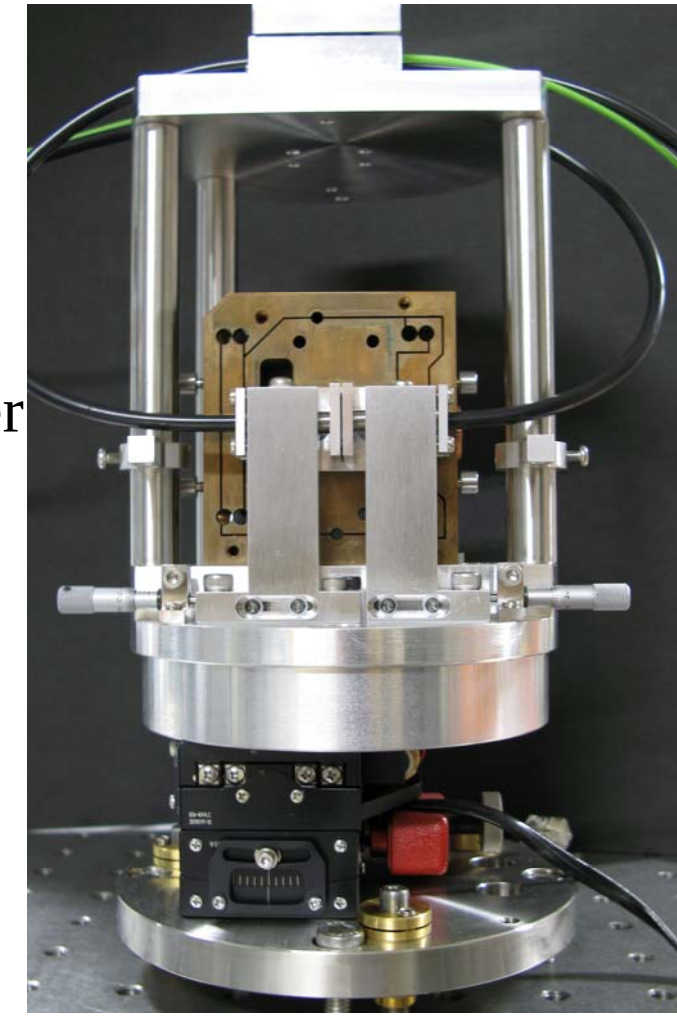

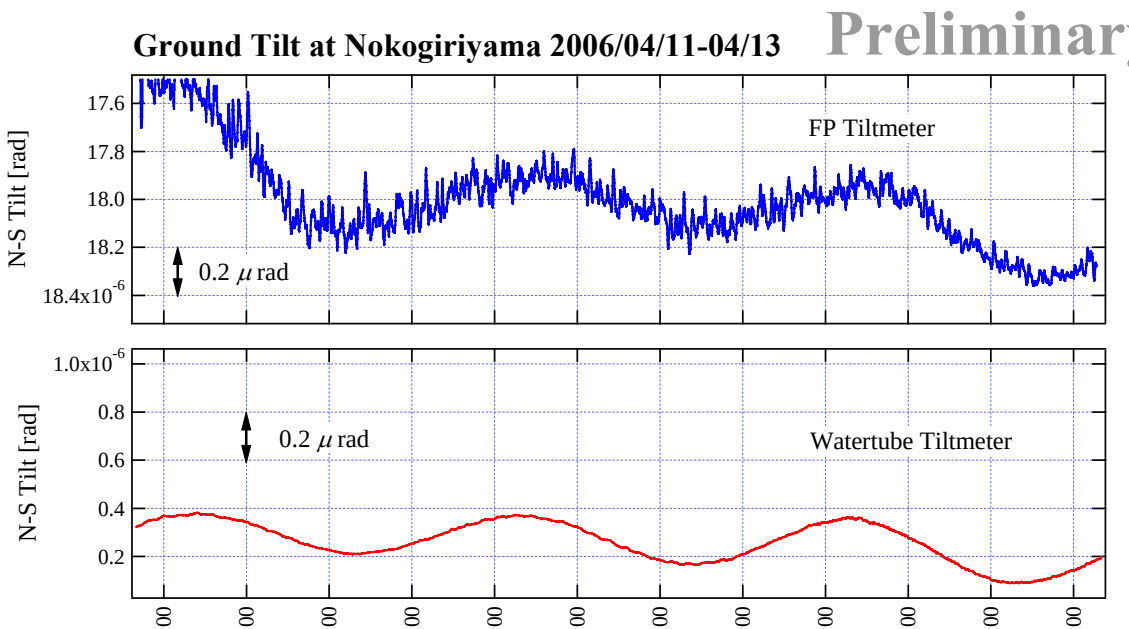

Vertical accelerometer

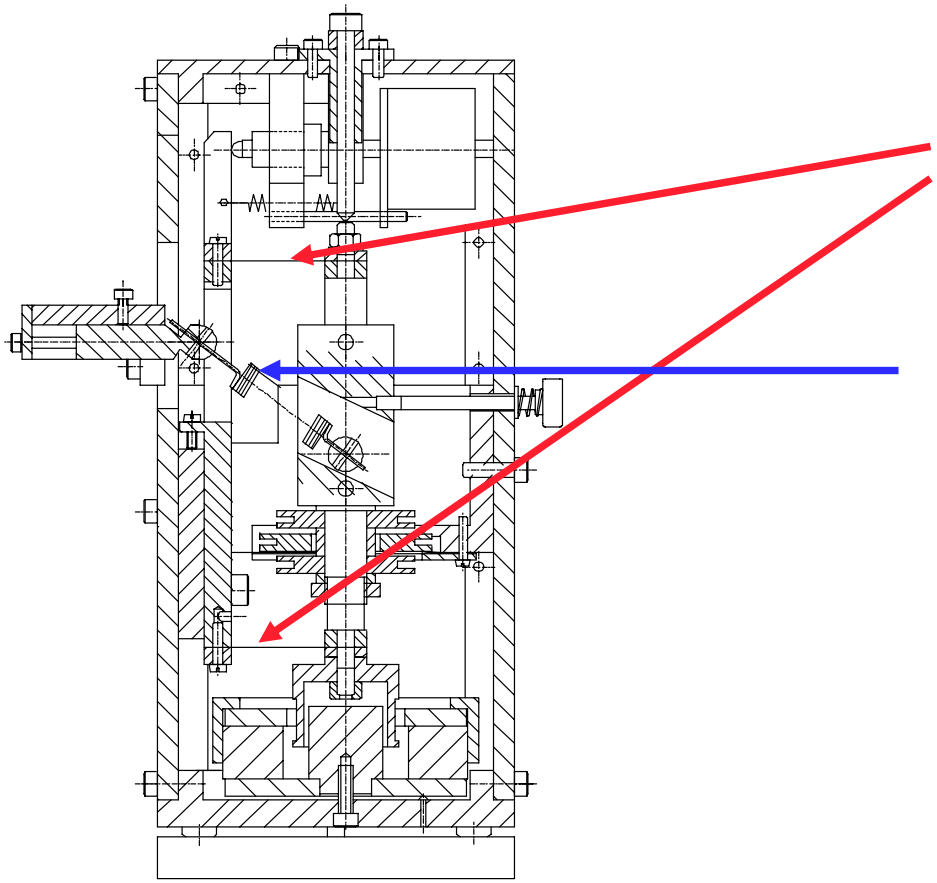

- Flex joint pair to constraint to vertical movement
- Lacrosse spring for lift and frequency tuning

Vertical accelerometer

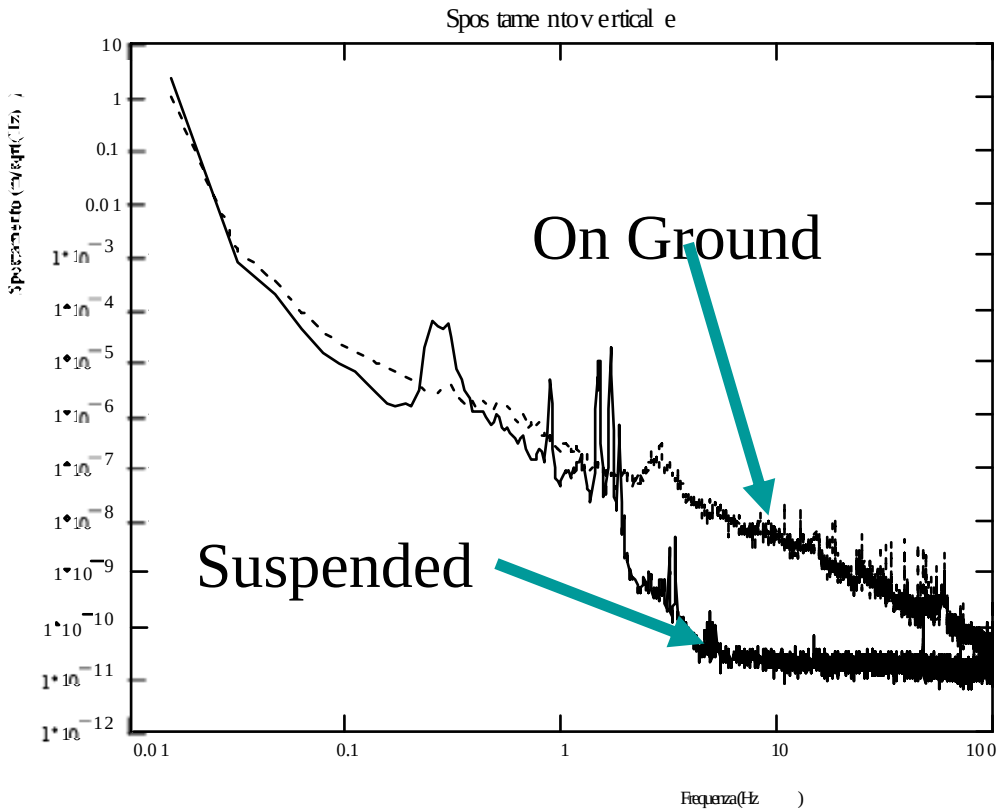

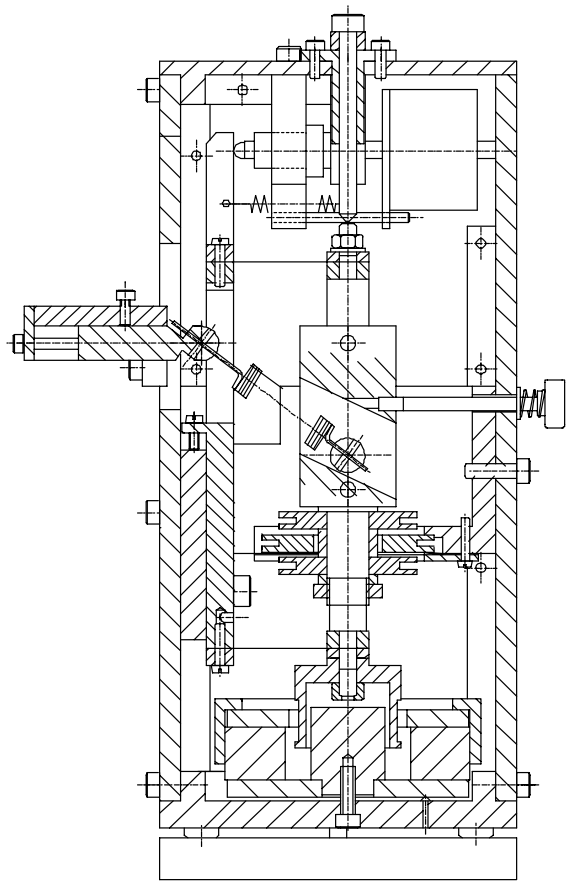

Vertical accelerometer

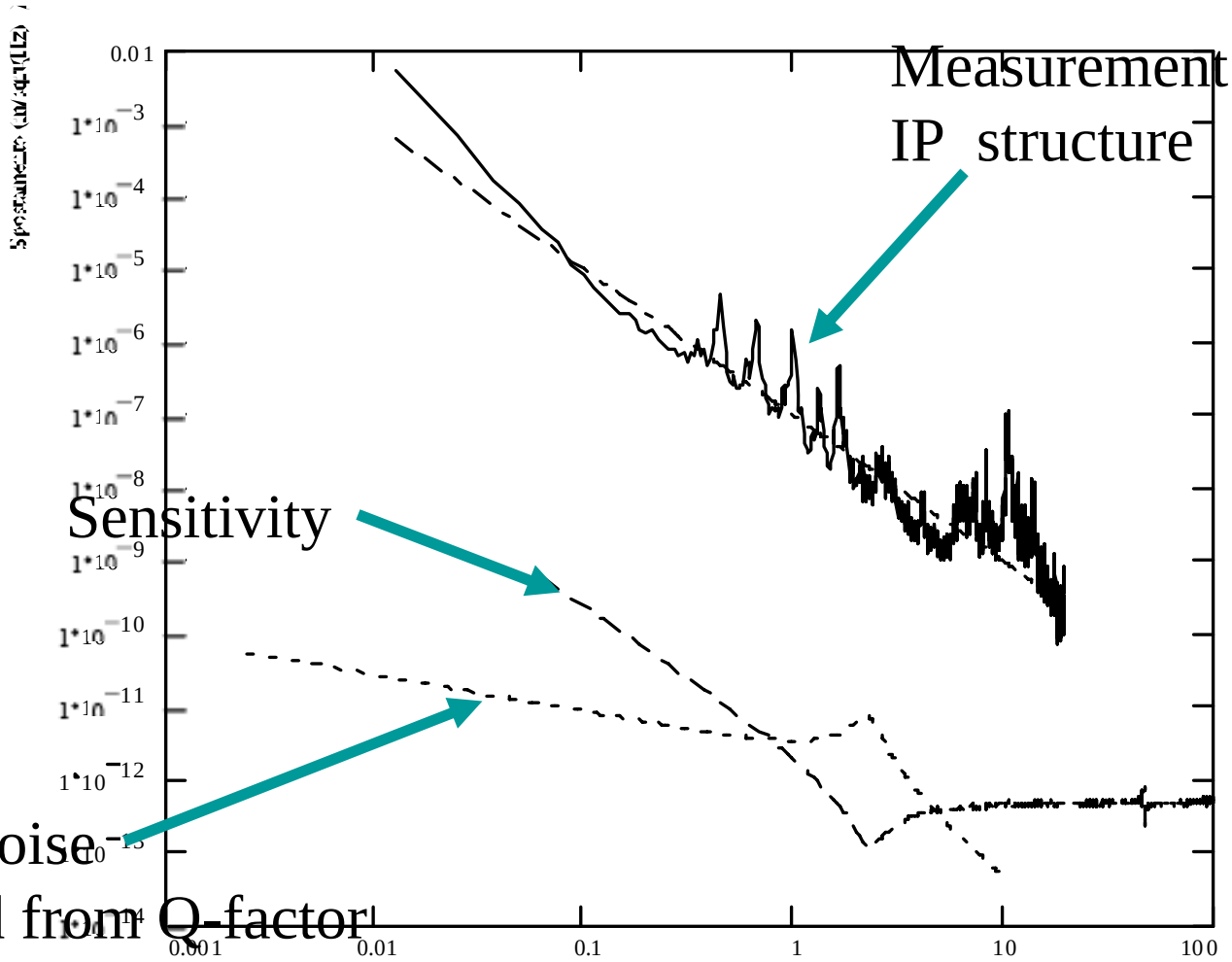

Vertical accelerometer next development

- Bertolini
- The GAS springs

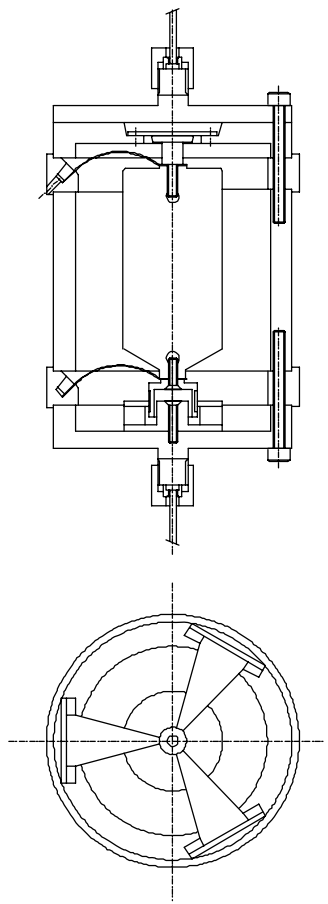

Geometric anti-spring vertical accelerometer -I-

A concept prototype of a companion vertical accelerometer with the sensing mass suspended by means of a double geometric anti-spring (GAS) system was built.

The monolithic GAS springs were machined by photochemical etching from a 0.1 mm thick foil of precipitation hardened CuBe. The mechanical resonant frequency could be lowered down to 0.3 Hz adjusting the compression of the spring system.

Force balance operation is achieved with differential capacitance position sensing and linear feedback actuator.

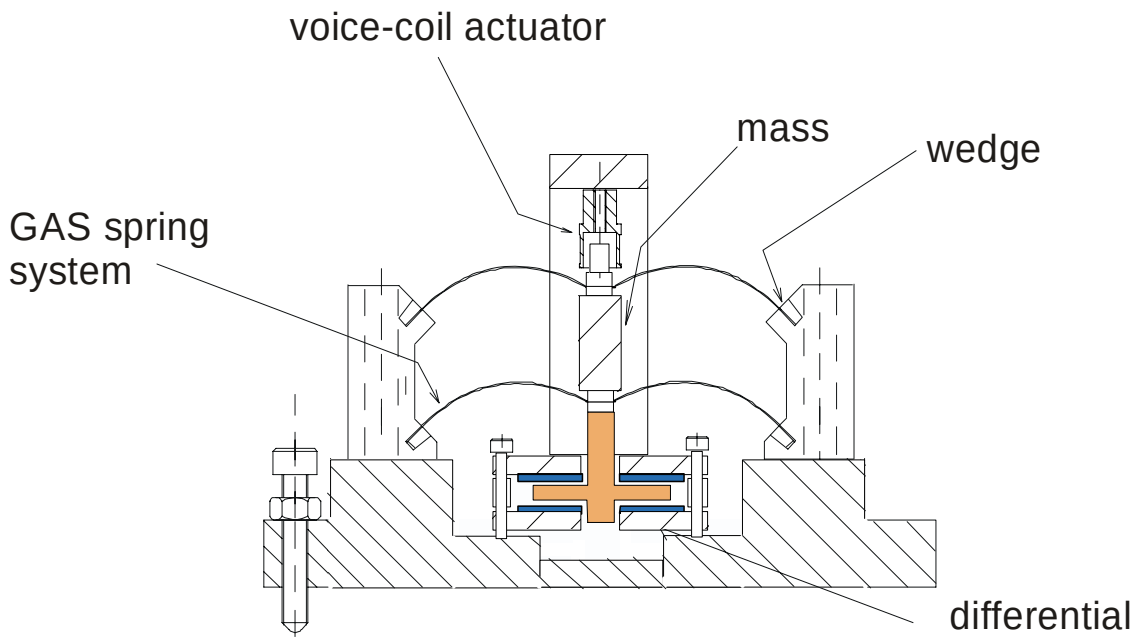

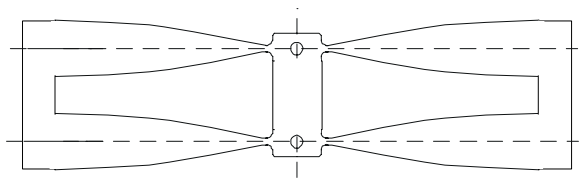

monolithic double GAS spring (top view)

A. Bertolini, N. Beverini, G. Cella, R.DeSalvo, F. Fidecaro, M. Francesconi, D. Simonetti, NIM A, 518 (2004) 233-235

LIGO

Geometric anti-spring vertical accelerometer -II-

Measured mechanical response of the prototype with natural period tuned to 0.7 sec.

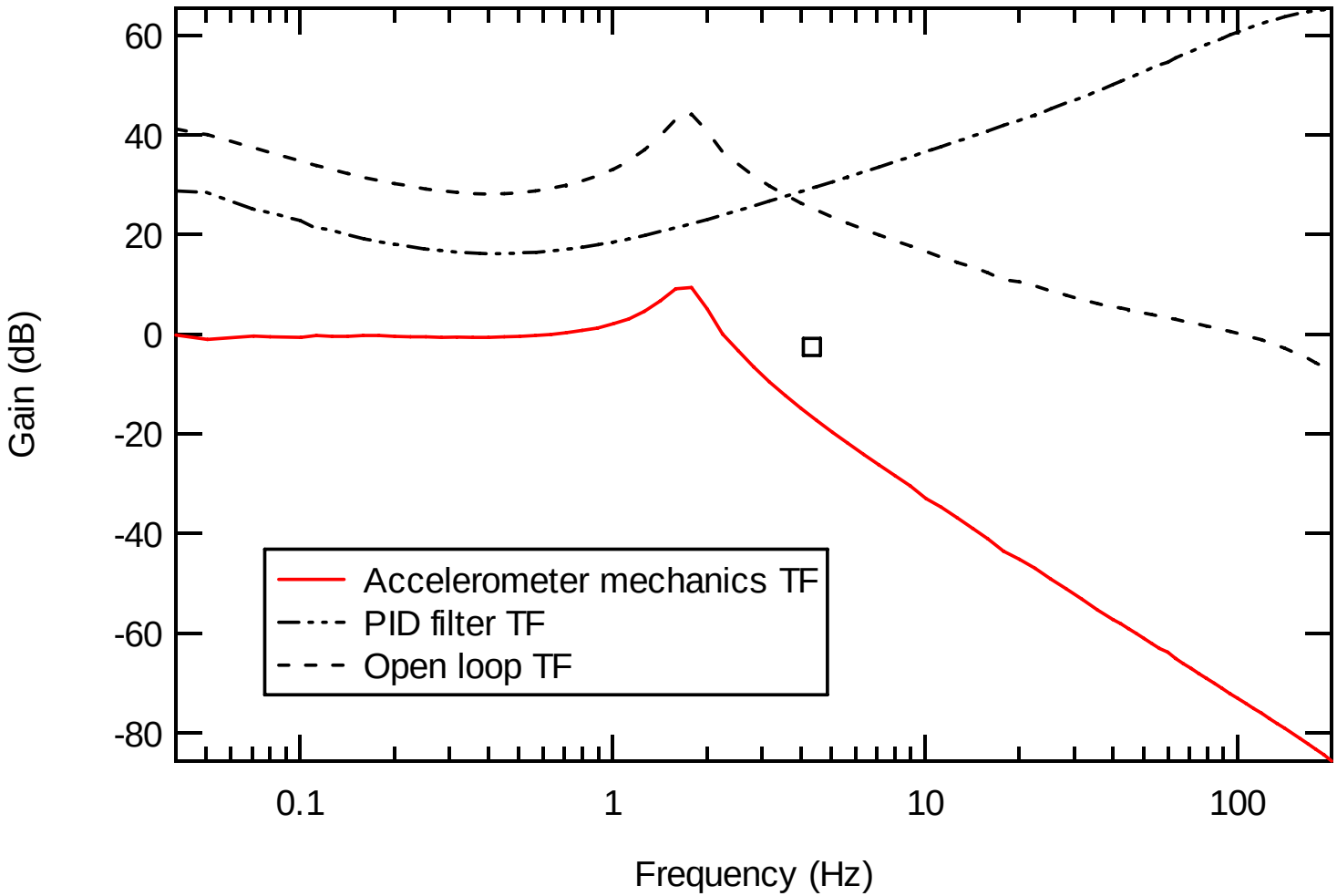

The double parallel spring geometry makes the sensor strongly reduces cross-axis (torsion and horizontal) sensitivity. No spurious resonances found below 300 Hz (see red line).

Tiltmeter developments

The first Virgo Tiltmeter ("96)

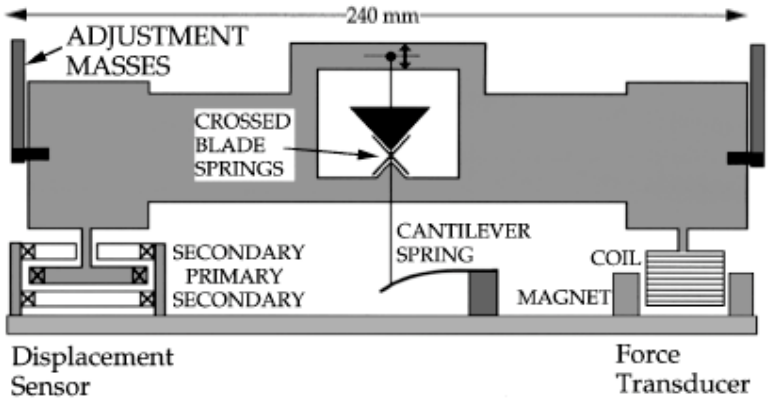

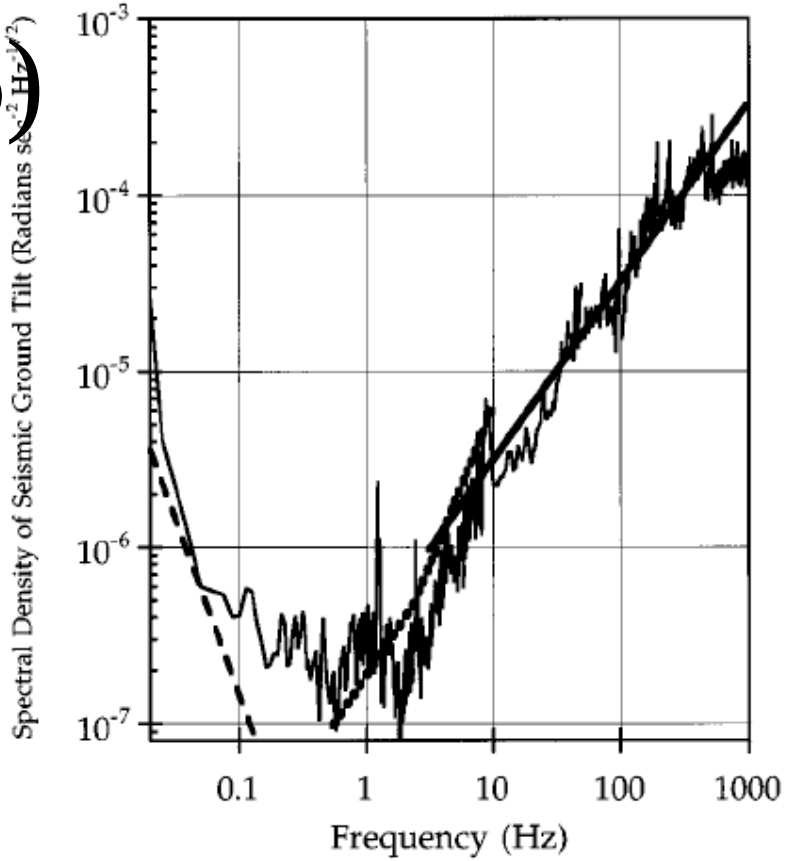

Ground tilt seismic spectrum measured rotational accelerometer

A. N. Luiten

Et al.

Rev. Sci. Instrum. 68 (4), April 1997

FIG. 5. The ground tilt seismic spectrum measured using the rotational accelerometer. The dotted line shows the measurements given in Ref. 5. The solid line shows the predicted level of ground tilt from the vertical seismic spectrum. The dashed line shows the contribution of residual horizontal acceleration sensitivity of the accelerometer.

LIGO

The second Virgo tilmeter (1998)

- Pisa-Florence group
- Symmetric sensing and actuation
- Shown 1/f Low Frequency Noise

The third Virgo tilt meter (work in progress)

- Pisa, Giazotto et al.
- Roma Tor Vergata, Minenkov et al.

- Heavier version of the 10 year old prototype

Rekindled interest in tiltmeters

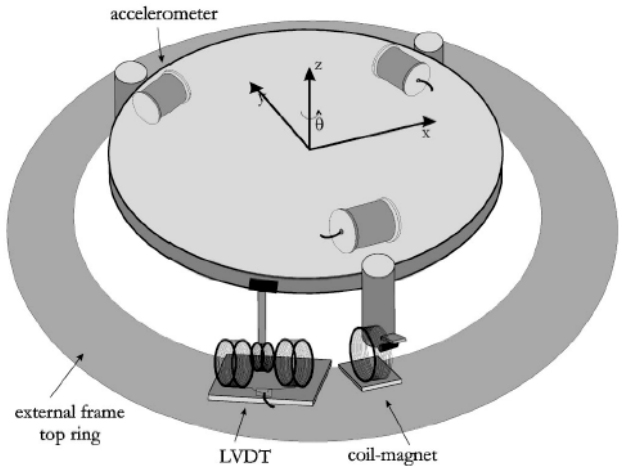

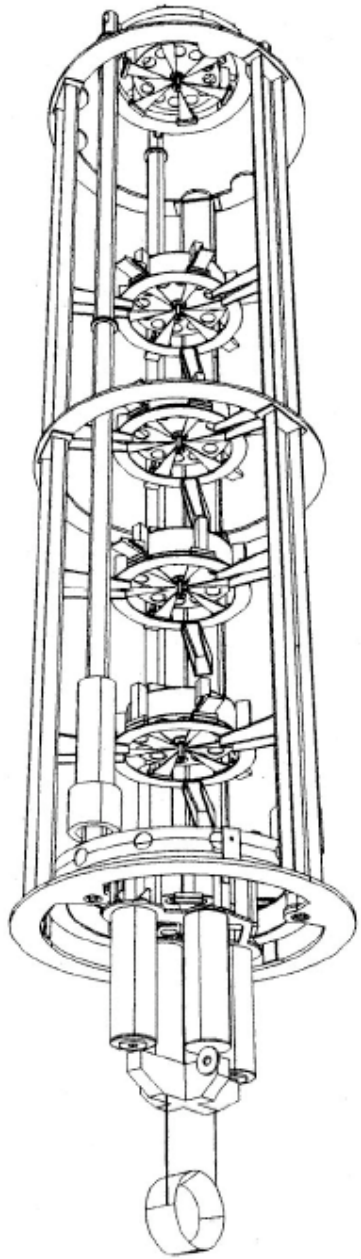

- Accelerometers on top of the IP are sensitive to tilt,
- Excess LF residual movement

Why tilt is suspected?

Experimental data

in the 100-200 mHz region is in better agreement with the

White noise Angular Acceleration simulations

and do not show the deep notch typical of the

White noise Displacement Acceleration simulations

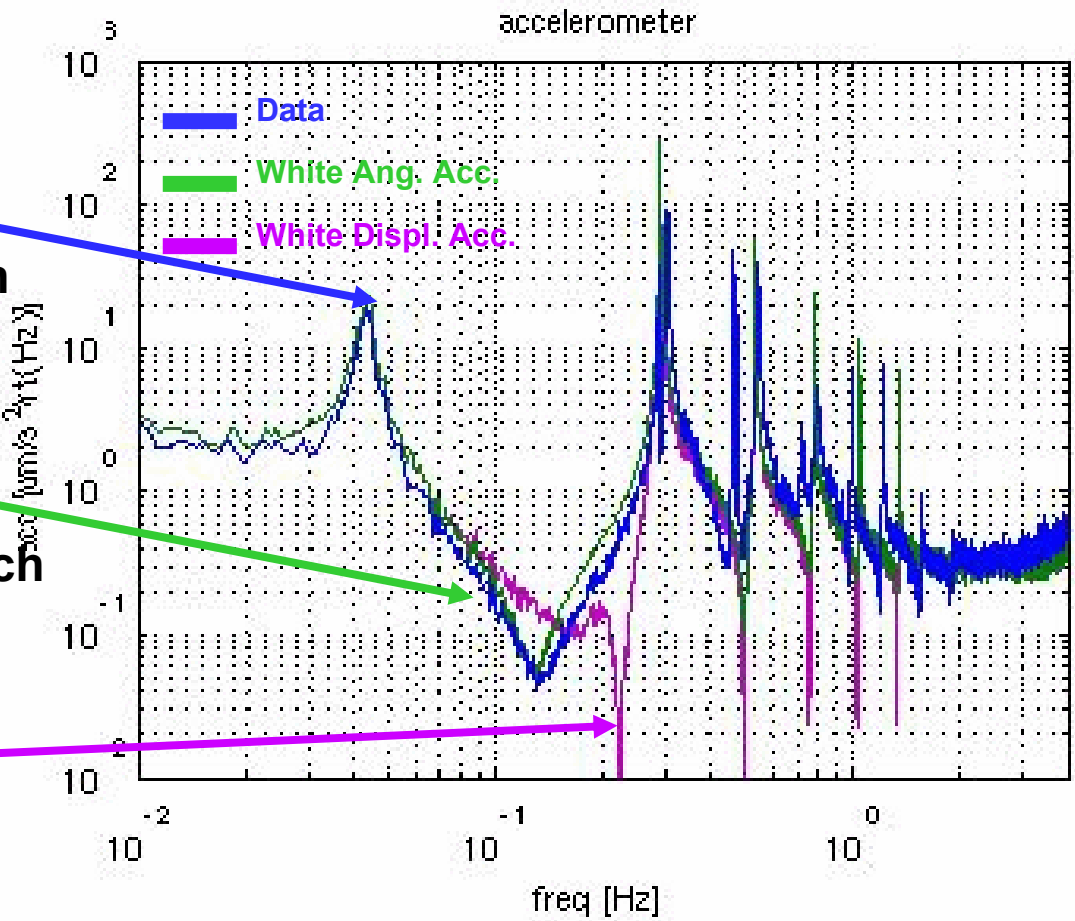

Desired Sensitivity of the Tilt Meter

This excess noise Signal on a windy day,

which fits the Data if it is Angular Acceleration,

is ~1μ/(s^{2}sqrt(Hz))

Therefore:

$$g \sin \tilde{\theta} = 10^{-6} \frac{m}{s^2 \sqrt{Hz}}$$

$$\tilde{\theta} \approx 10^{-7} \frac{rad}{\sqrt{Hz}}$$

Consequently the Tilt Meter sensitivity should stay in the range

$$10^{-9} \frac{rad}{\sqrt{Hz}} @ 100mHz$$

LIGO

TM conceptual design:

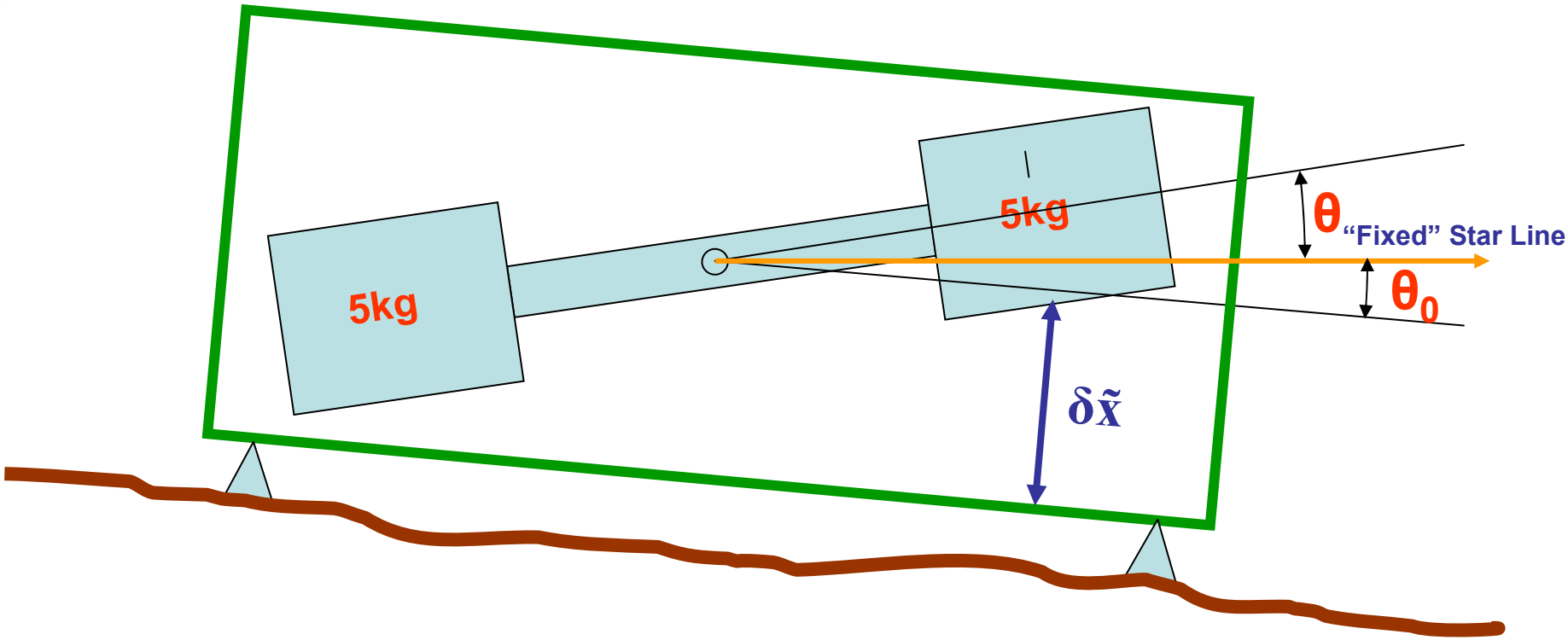

Tiltmeter prototype

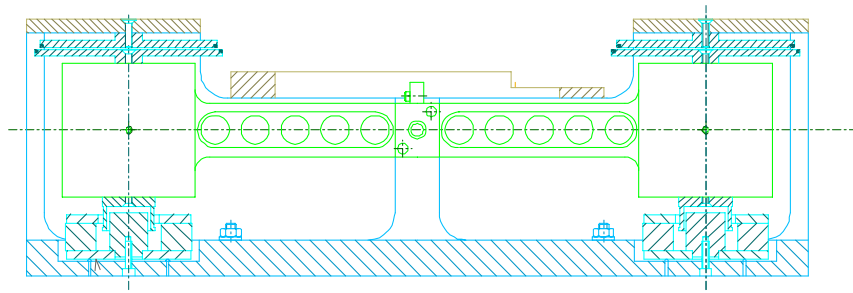

G070640-00-R

LIGO

Work in progress

If it confirms the preliminary data of the preceding prototype….

LIGO

The possible next tilt meter development

Advanced material flex joints

Steel alloys,
Tungsten
Niobium
Silicon
Silica. . . .

Prototype flexures

Carl Justin Kamp, Sean Mattingly

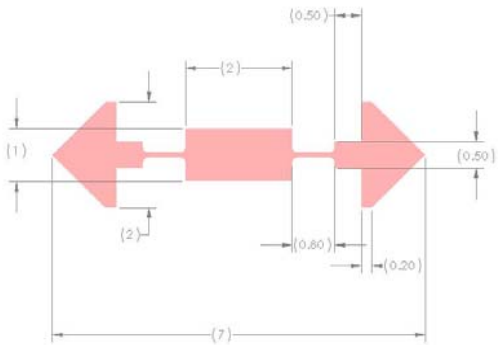

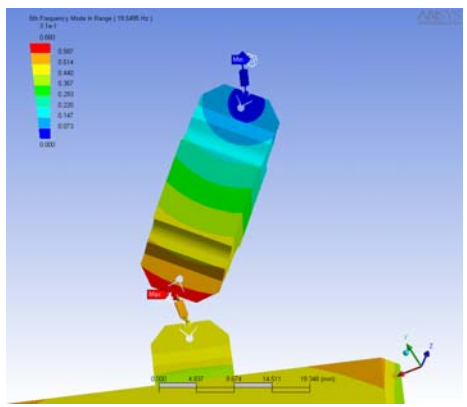

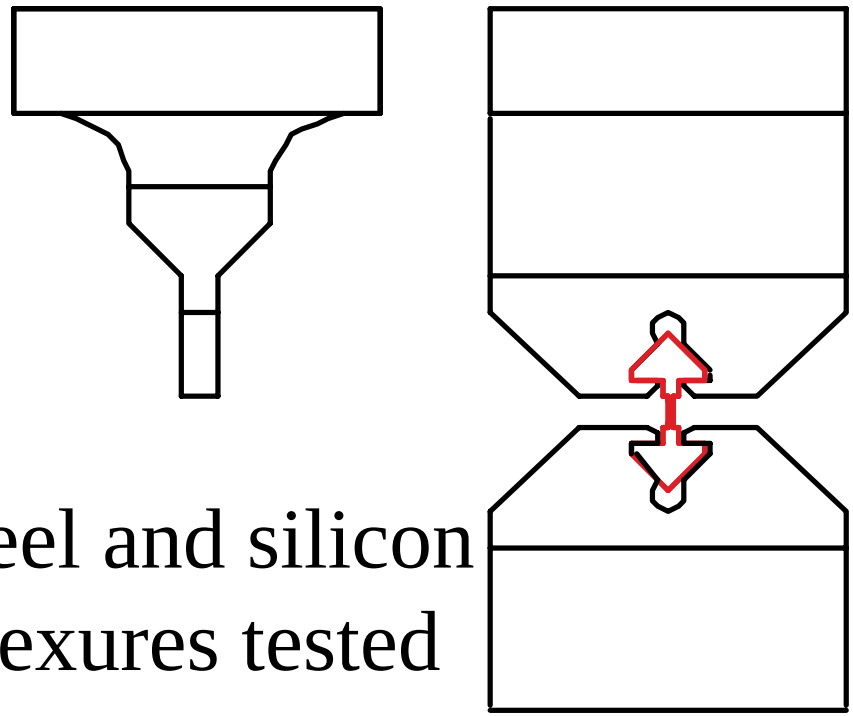

Steel and silicon flexures tested

LIGO

Q-Factor Analysis of Mono-Crystalline Silicon Flex Joints for Advanced LIGO

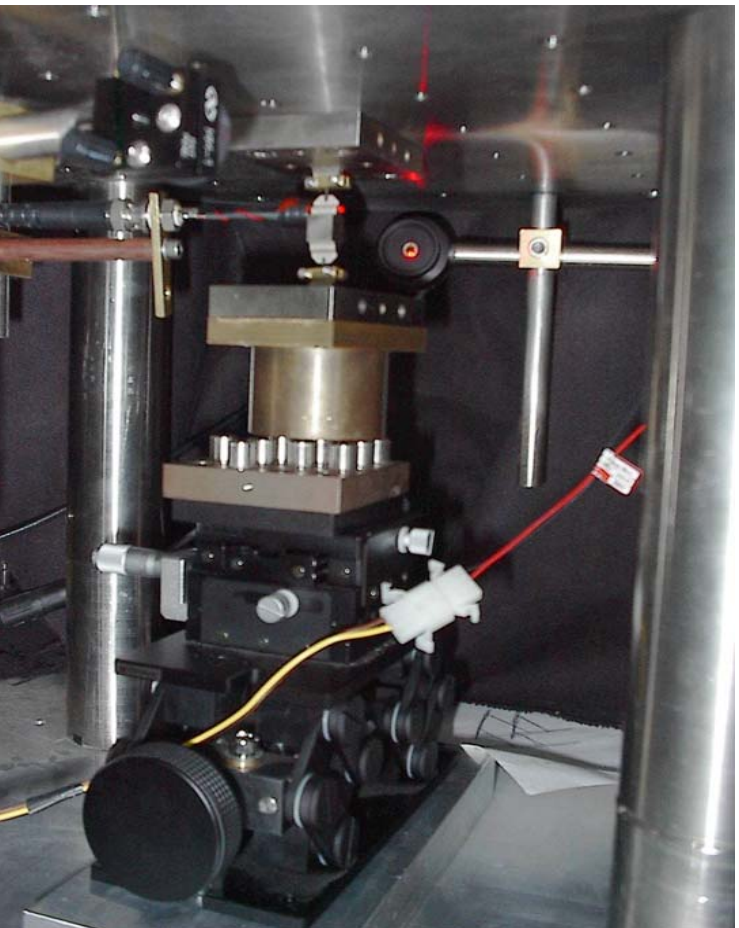

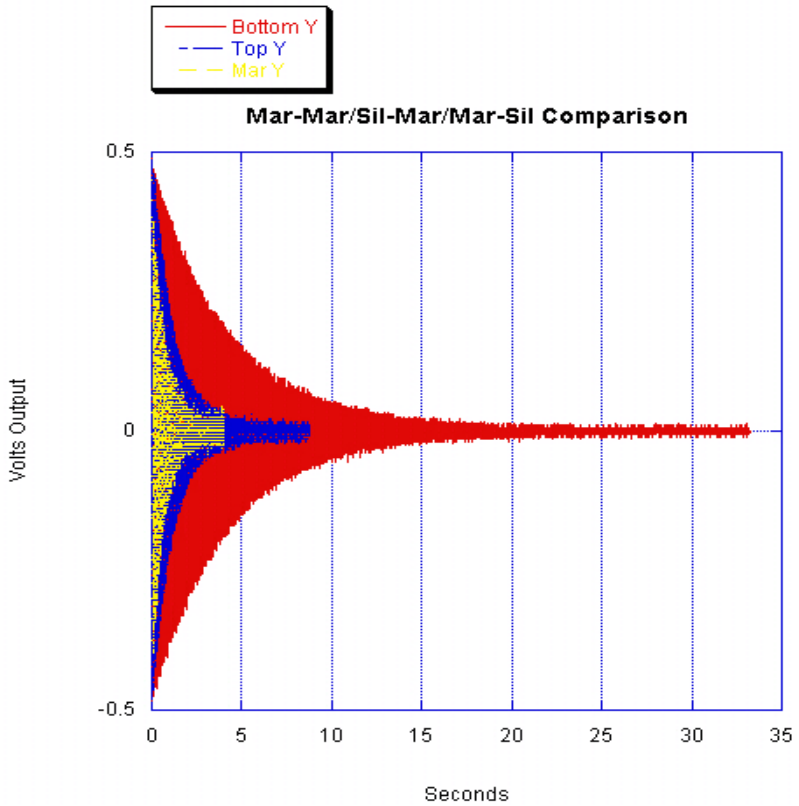

Hysteresis studies

Motivation:

1/f attenuation Problem emerging in the seismic attenuators

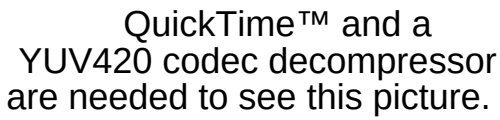
QuickTime™ and a
YUV420 codec decompressor
are needed to see this picture.

Hysteresis studies

Maddalena Mantovani

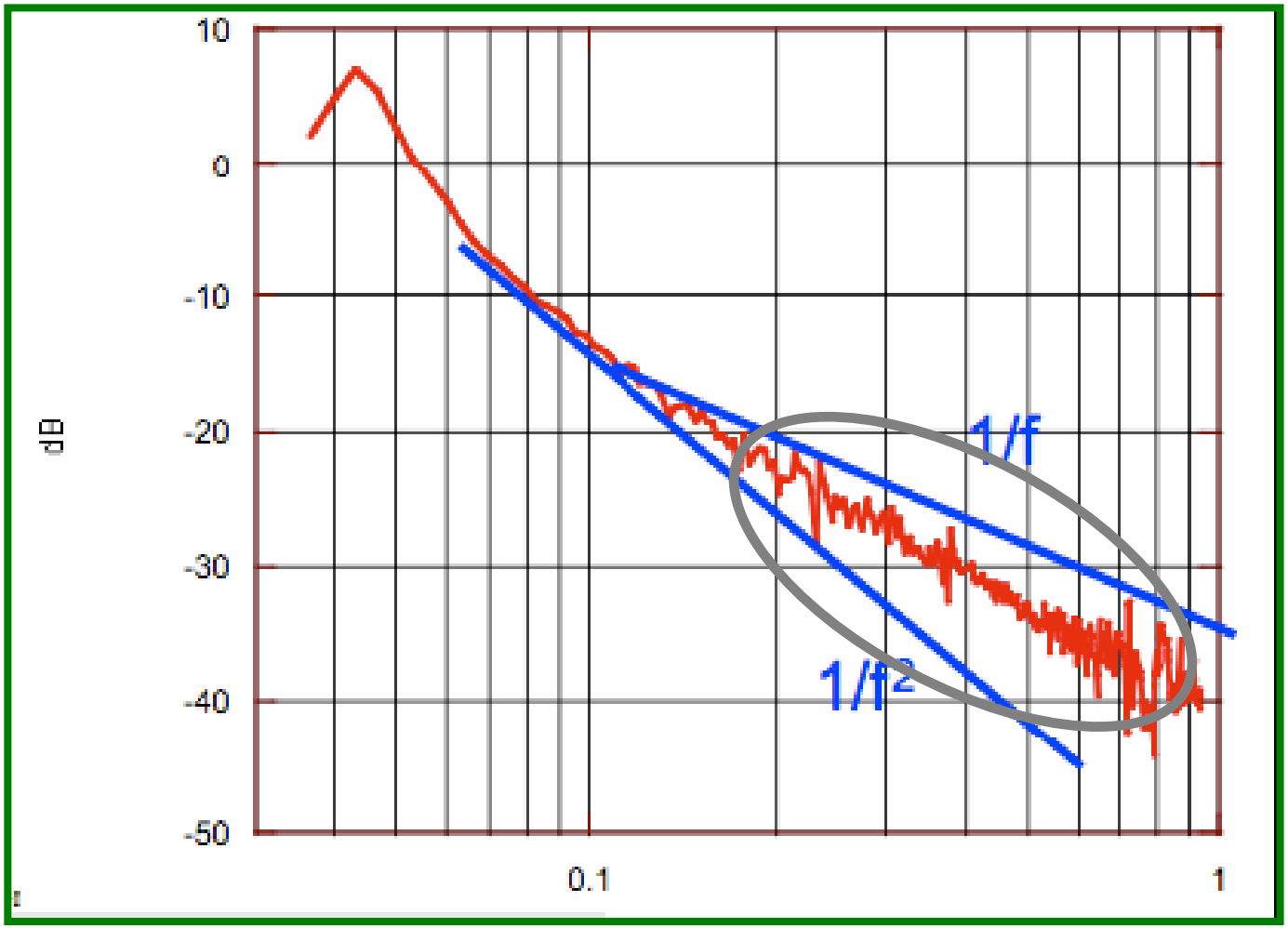

M. Mantovani, R. DeSalvo, *One Hertz Seismic Attenuation for Low Frequency Gravitational Waves Interferometers*, accepted for publication on Nucl. Instr. and Meth. (2005).

Hysteresis studies

Alberto Stochino

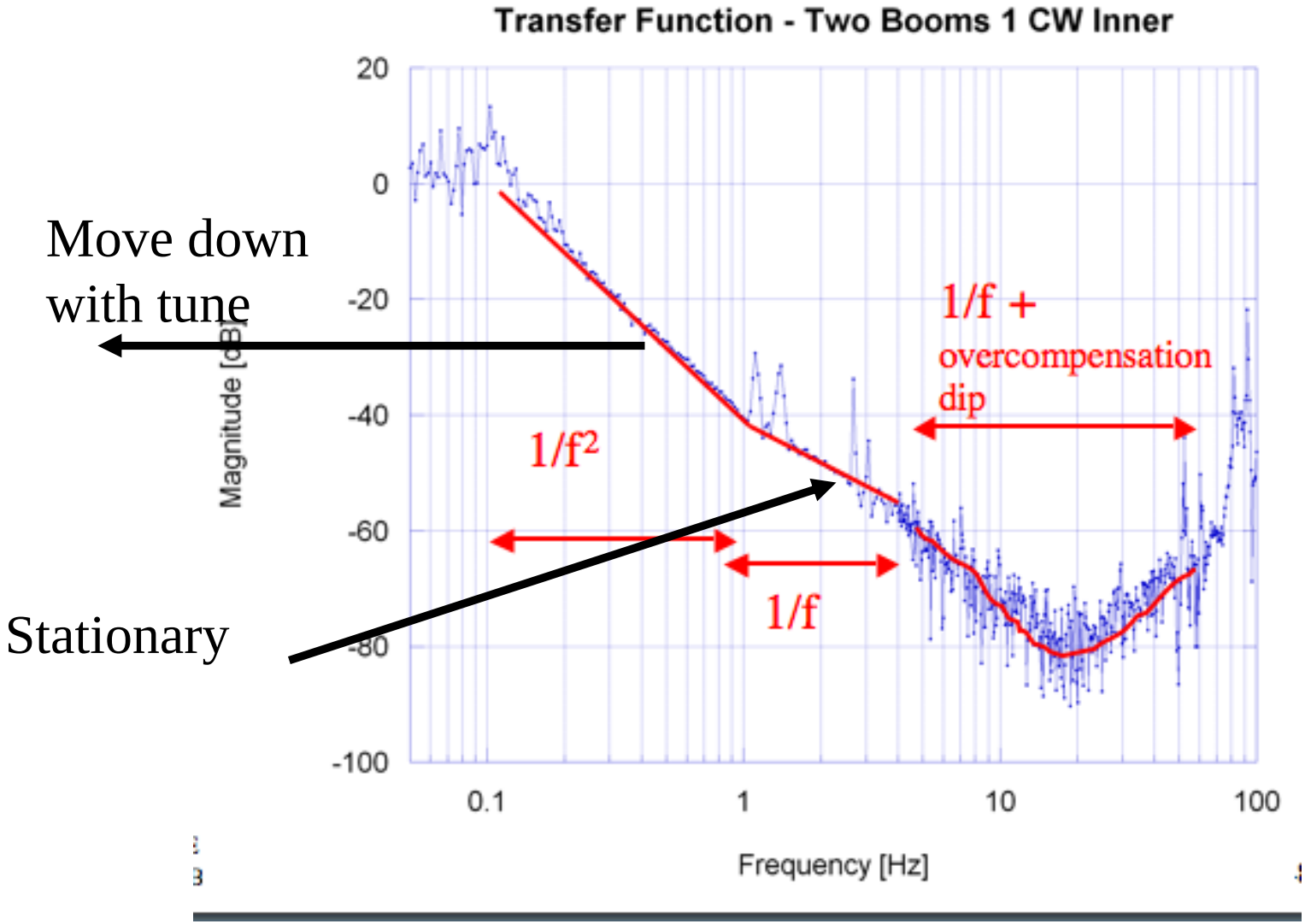

A. Stochino, *Performance Improvement of the Geometric Anti Spring (GAS) Seismic Filter for Gravitational Waves Detectors*, SURF-LIGO 2005 Final Report, LIGO-P050074-00-R.

Hysteresis studies

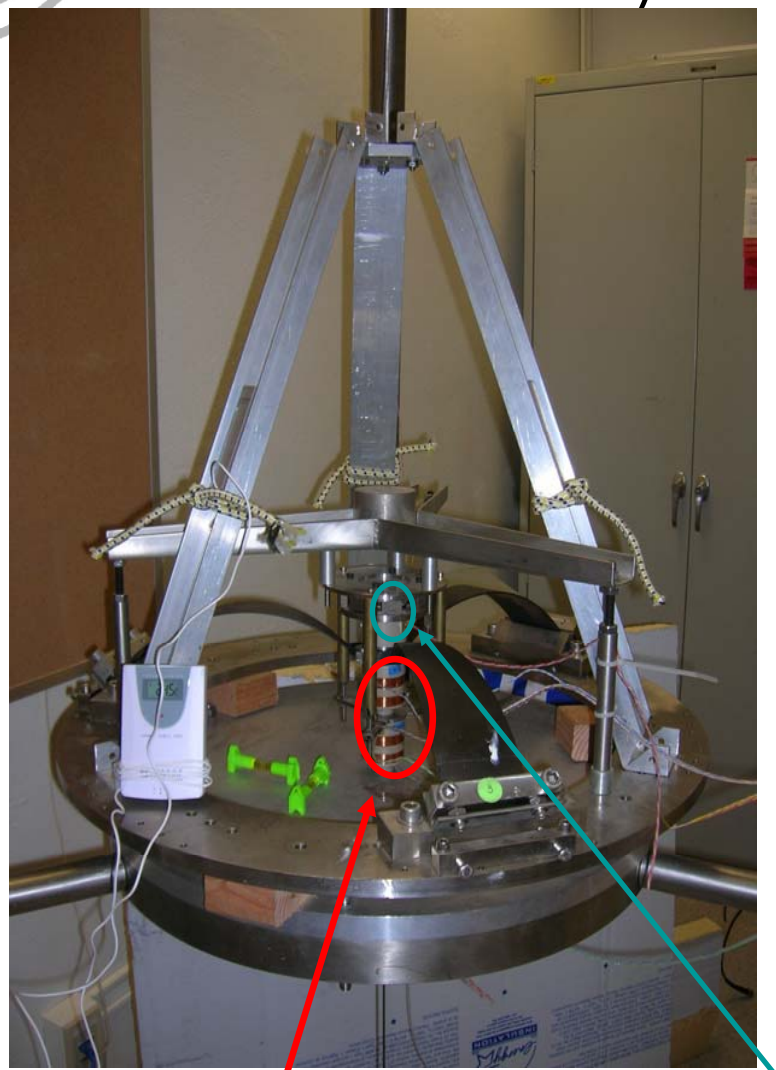

Method:

- Geometric Anti Spring geometry reduces resonant frequency (0.2 Hz) and elastic recall force thus exposing hysteresis

- Excite the attenuator using a coaxial Actuator
  1. With a slow pulse
  2. With a sinusoid

- Read the position with LVDT

Hysteresis studies pulse excitation

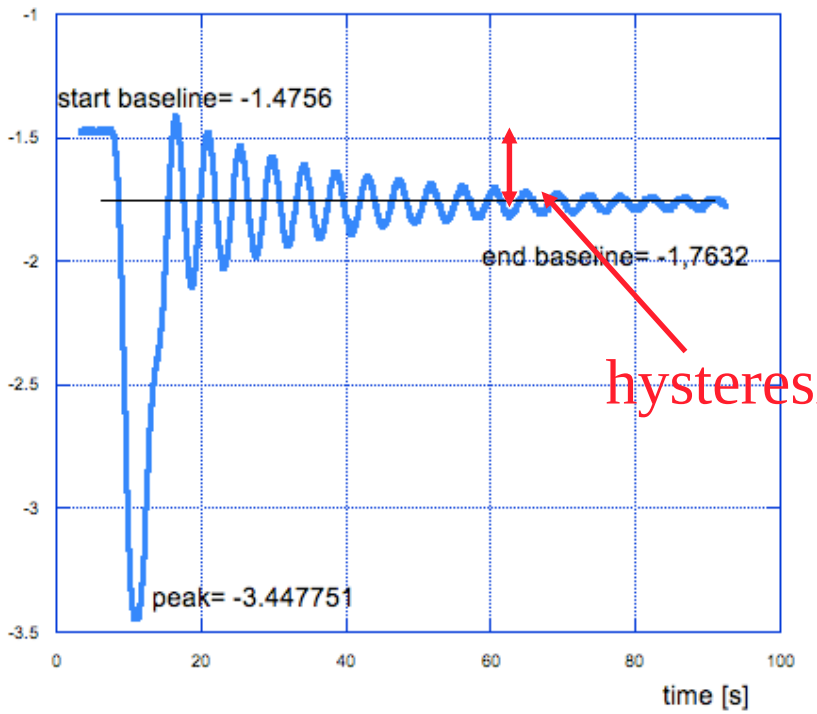

hysteresis

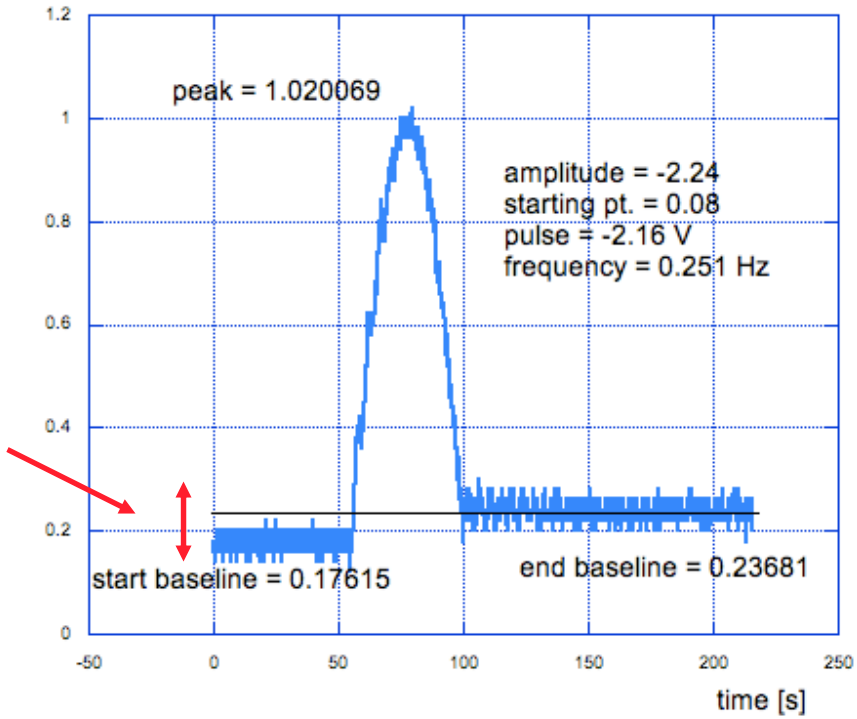

Hysteresis studies pulse excitation

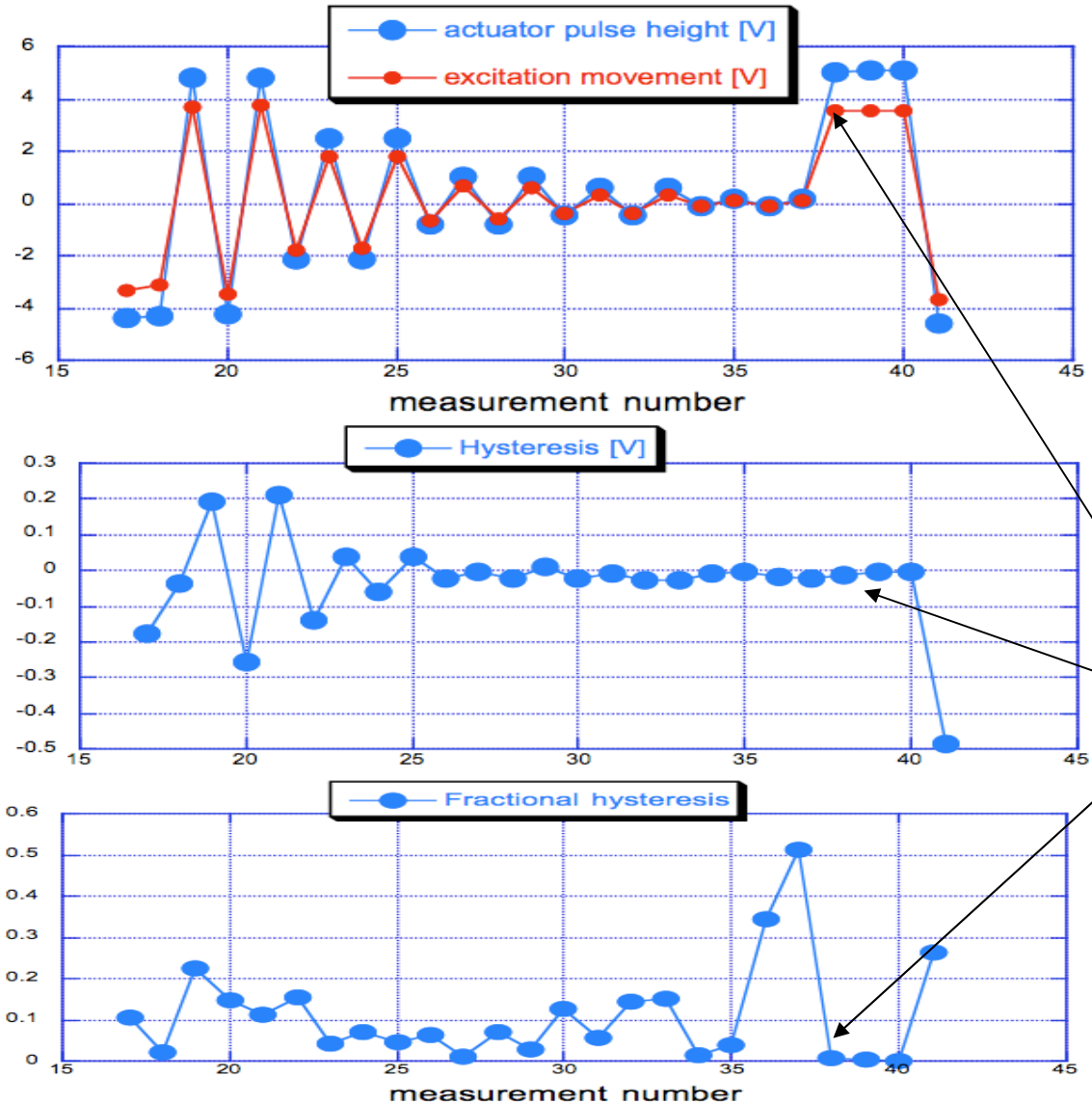

Arianna DiCintio
Maria Sartor

What happens to hysteresis here?

Hysteresis studies

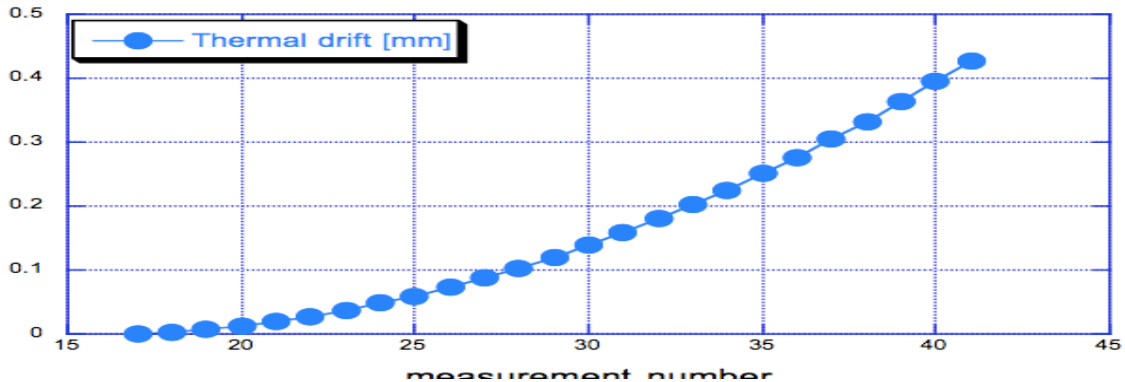

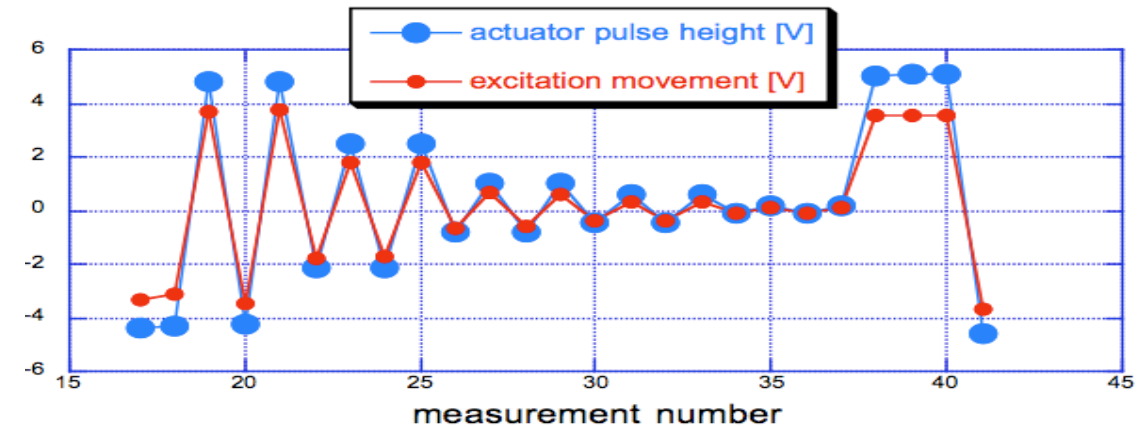

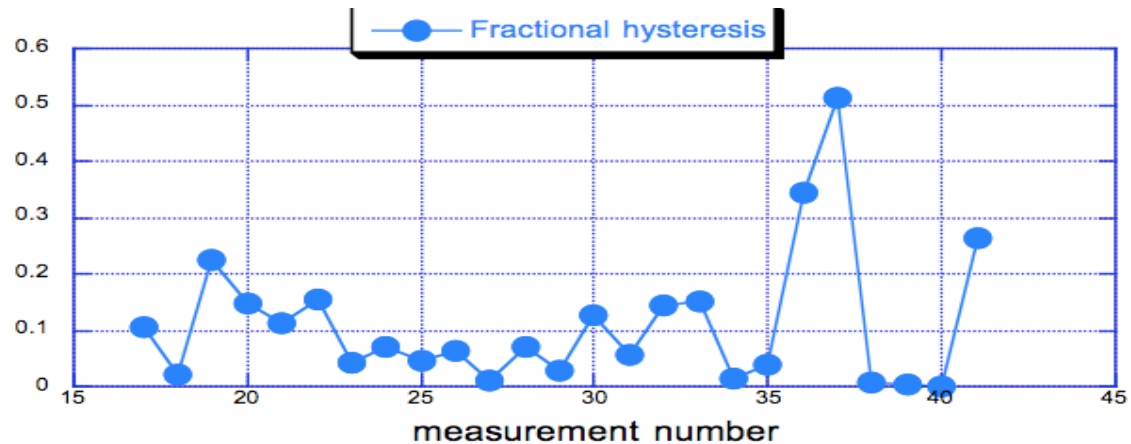

(Calibration about 1.23 mm/V)

Thermal
Drift equivalent to
an excitation pulse.

Overwhelms
Hysteresis in its
Direction
Enhances it the
Opposite direction

Implications of Hysteresis studies

pulse excitation results

- All movements of the system contribute to hysteresis pile up.
- If hysteresis at higher frequencies is the source of the low frequency 1/f excess noise
- During earthquakes the amplitude of the LF excess noise must also grow with HF amplitude

- The Low Frequency component may not stick out of the LF noise curve measured in quiet times

Hysteresis studies sinusoid excitation

Use the setup in an effort to quantize the problem

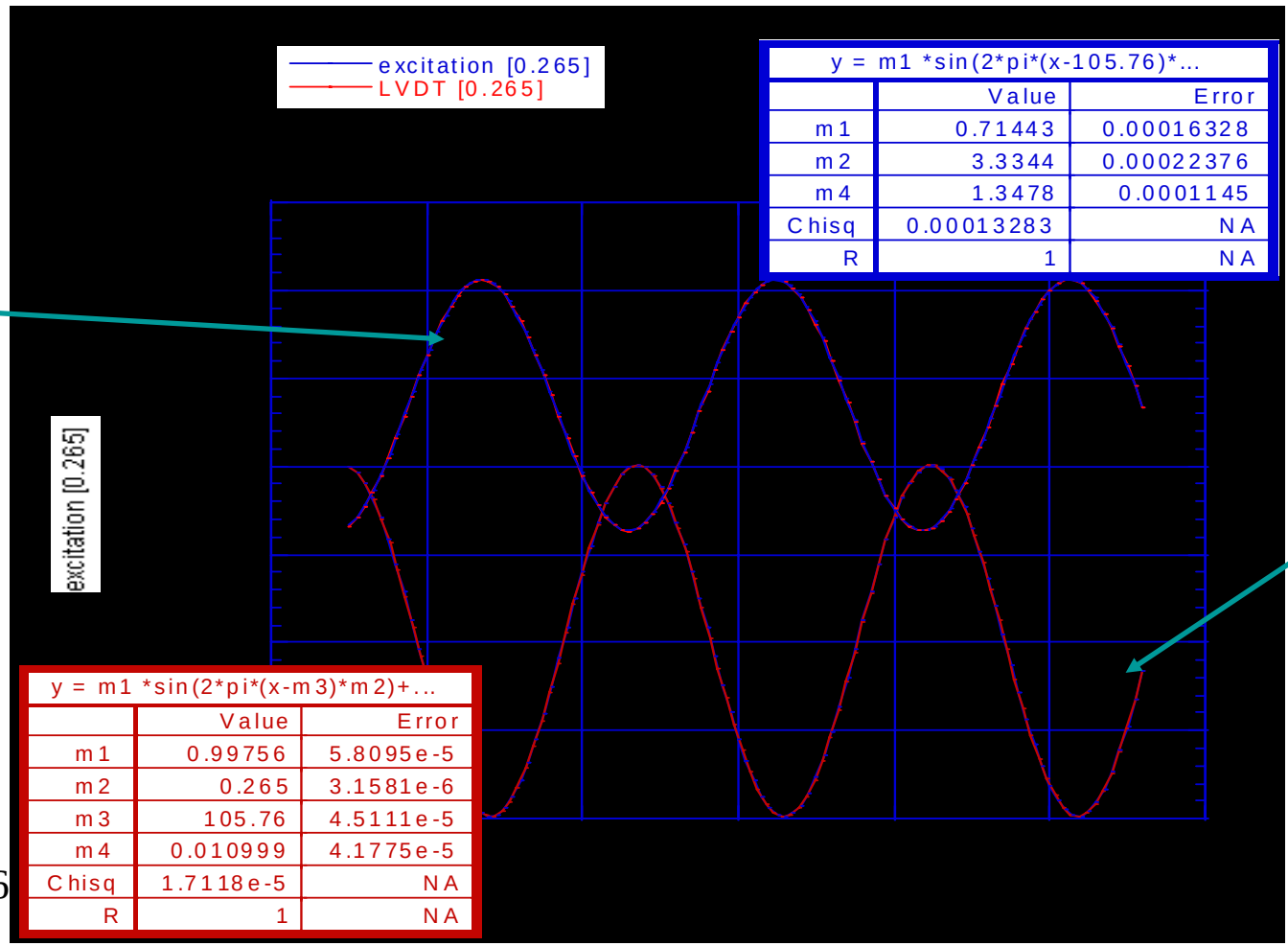

LVDT Position Signal[V]

Excitation[V]

- phase changing sign around the resonance
- Hysterisis loop through resonance

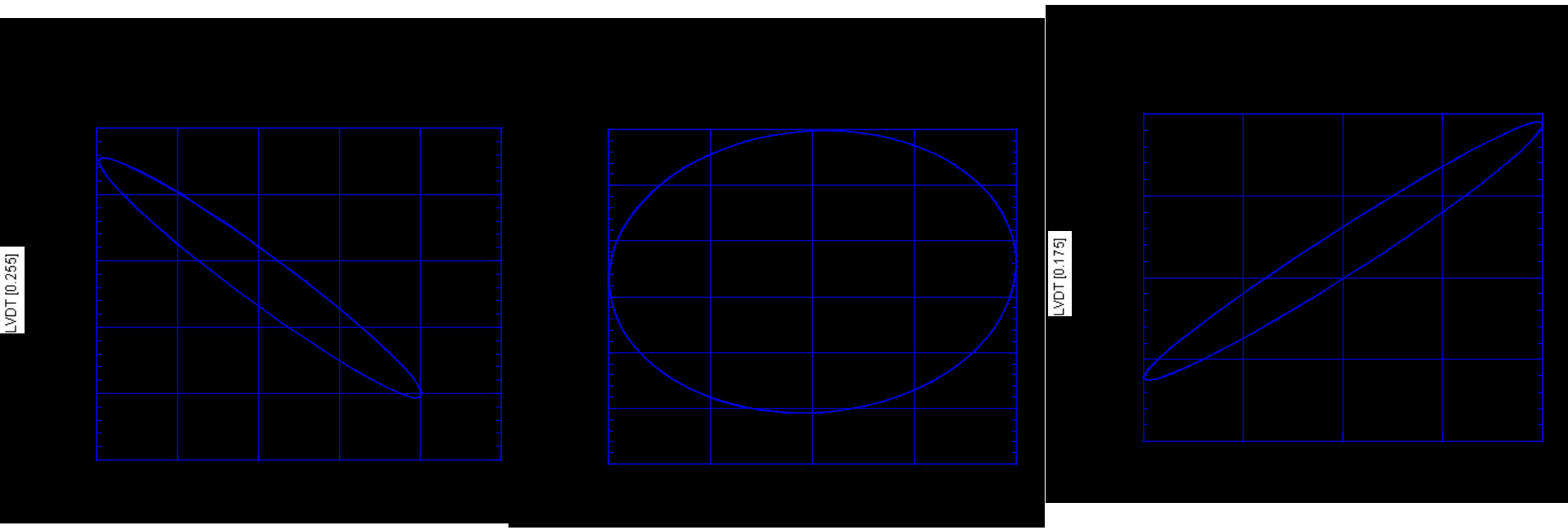

COMPARISON STEP UP/DOWN

- We expect different behaviors in large amplitude
- scan up and down

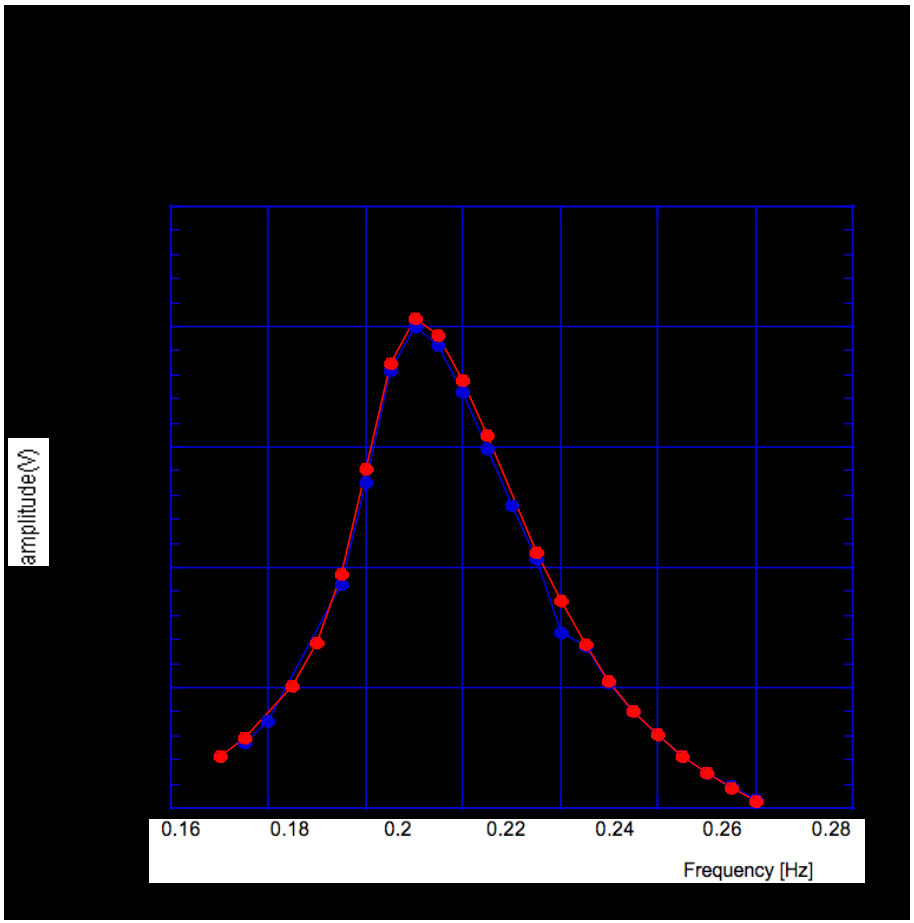

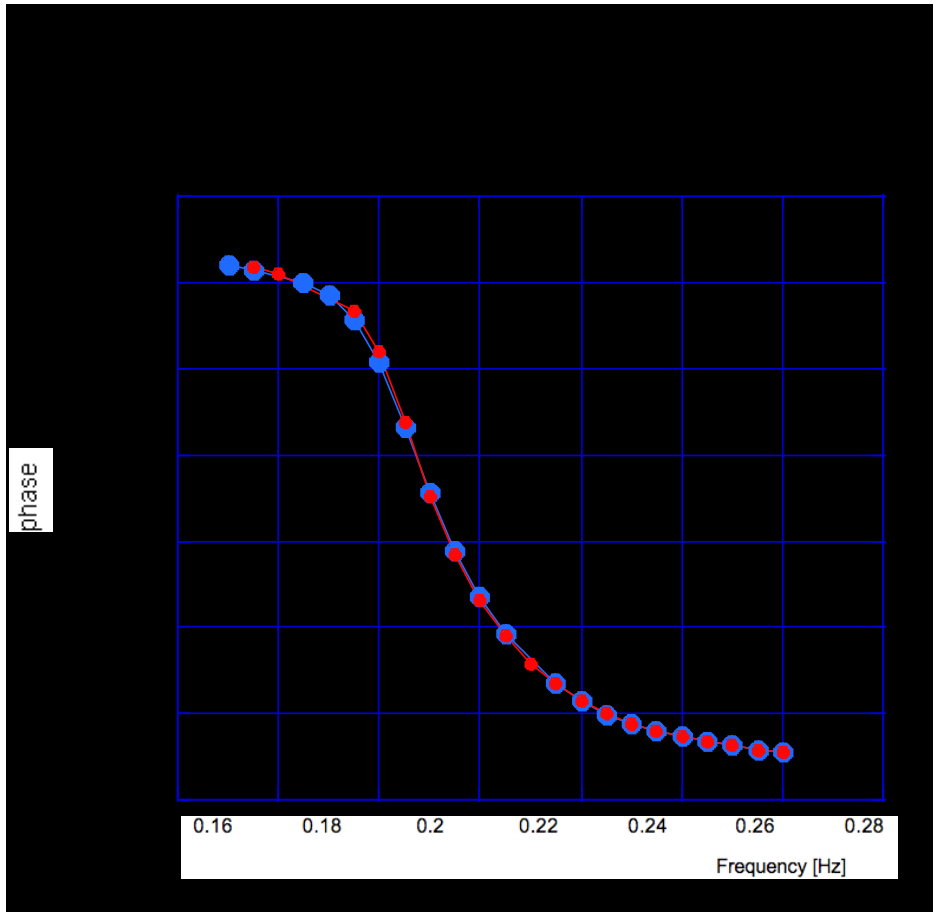

energy loss peaks at the resonance

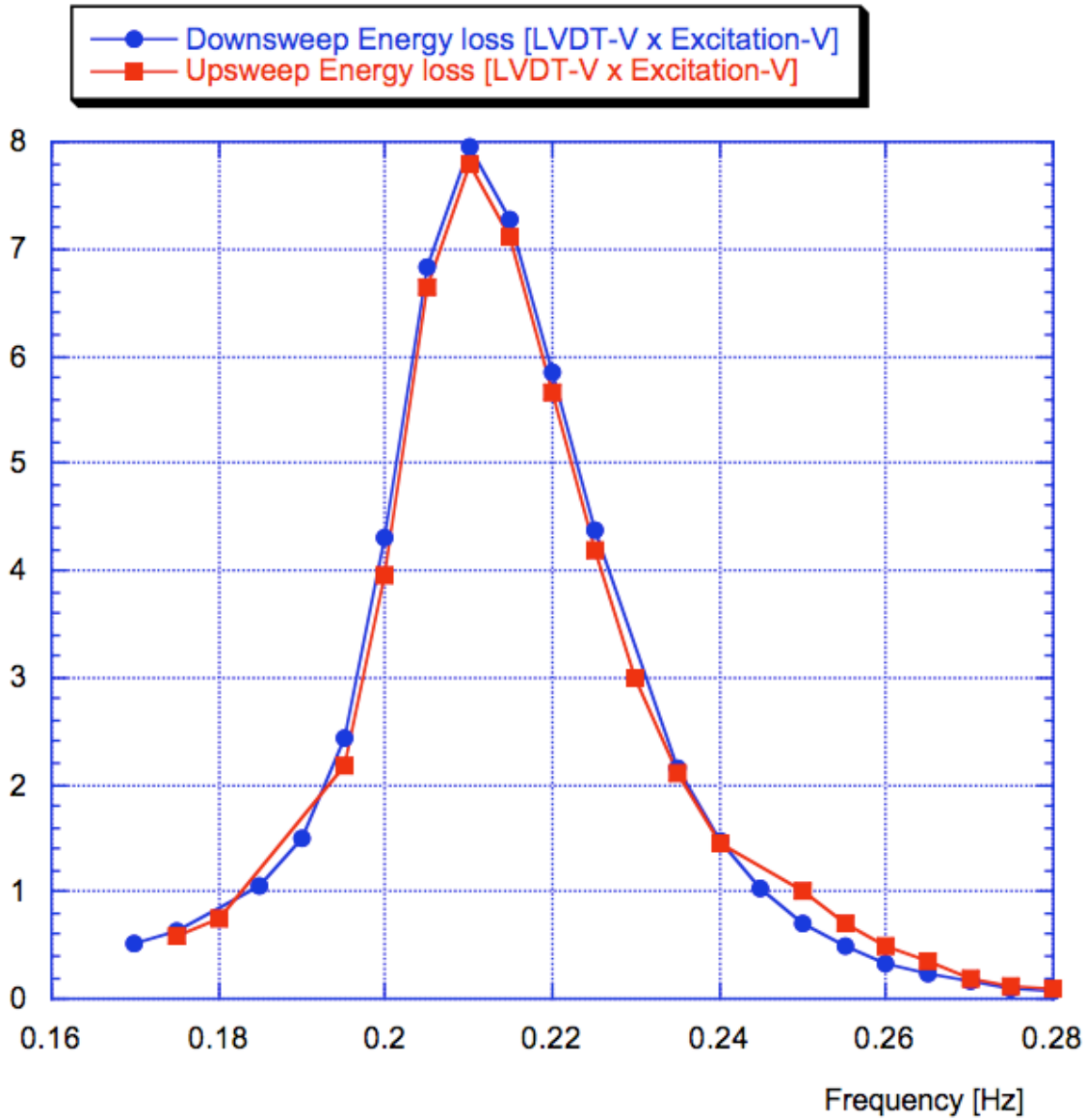

Hysteresis studies pulse excitation

- Is the measured amount of Hysteresis sufficient to explain the excess LF 1/fnoise?
- May play back some high frequency (>1Hz) noise in the system at various amplitudes and measure the LF frequency noise level
- Work in progress

Possible use of GW interferometers for seismology

- GW interferometers are not built for seismology.
- Still they are large yardsticks and may come useful

GW Interferometers as large scale seismometers

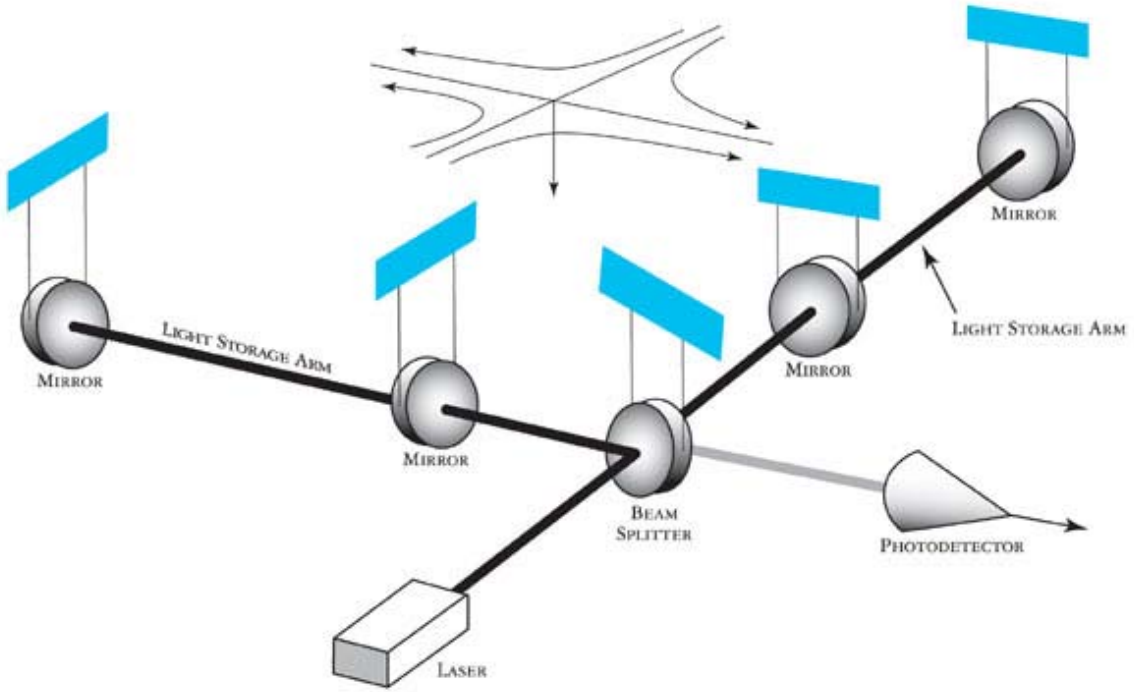

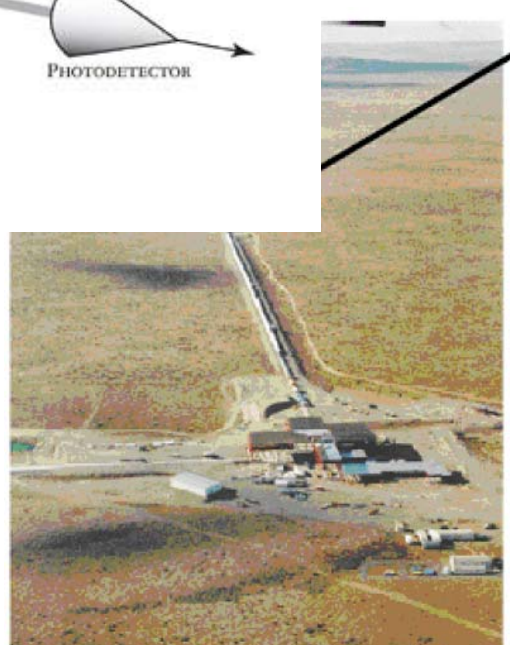

LIGO

- GW interferometers are 3-4 km long rigid yardsticks
- As long as lock is maintained its resolution is ~ 10^{-12}m

but with a difficult transfer function

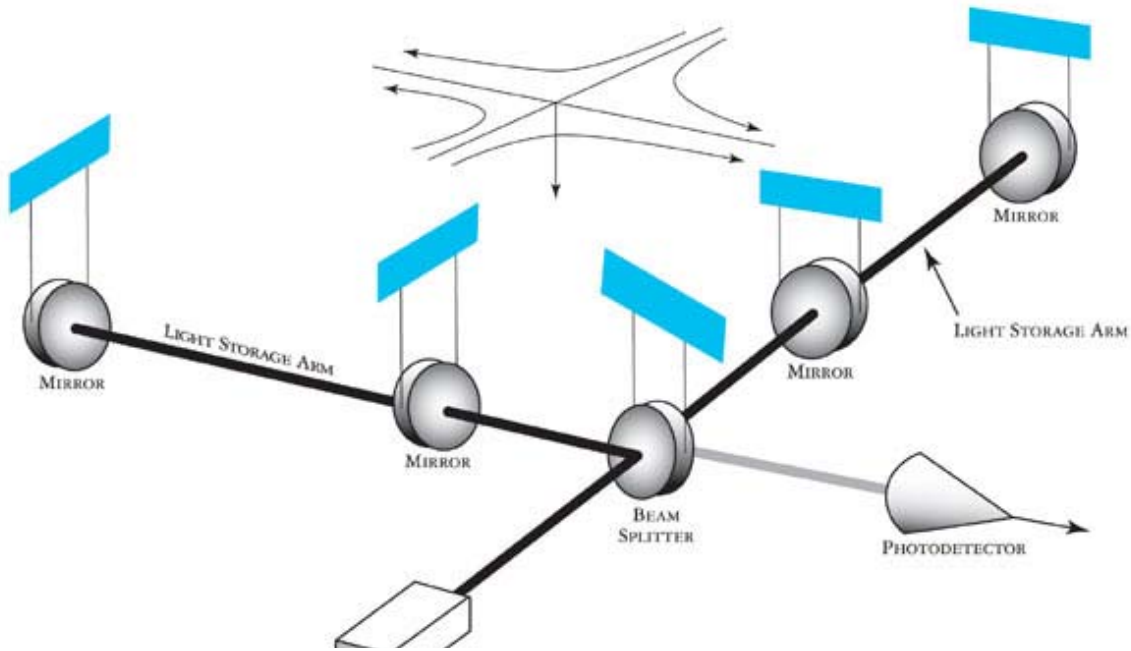

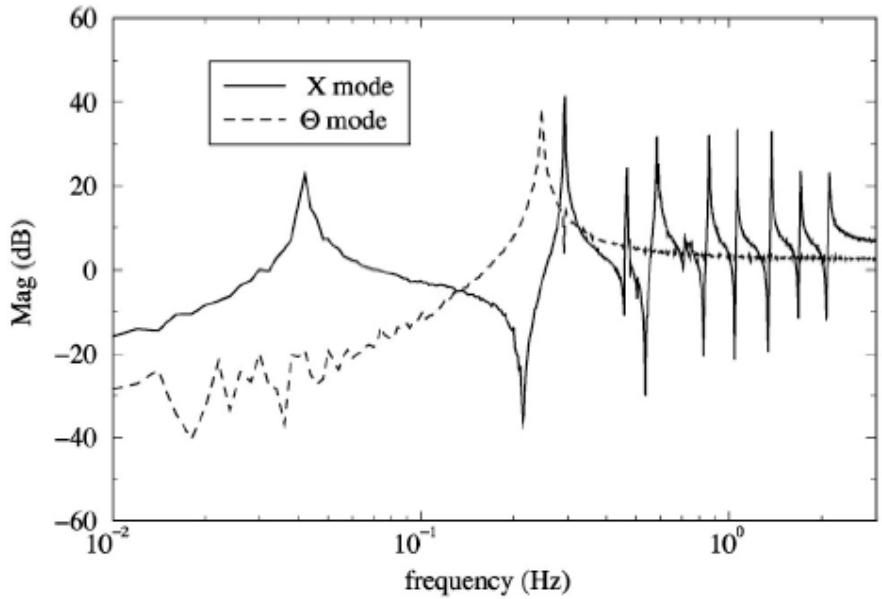

Seismic Strain in the IFO's DARM_CTRL Signal

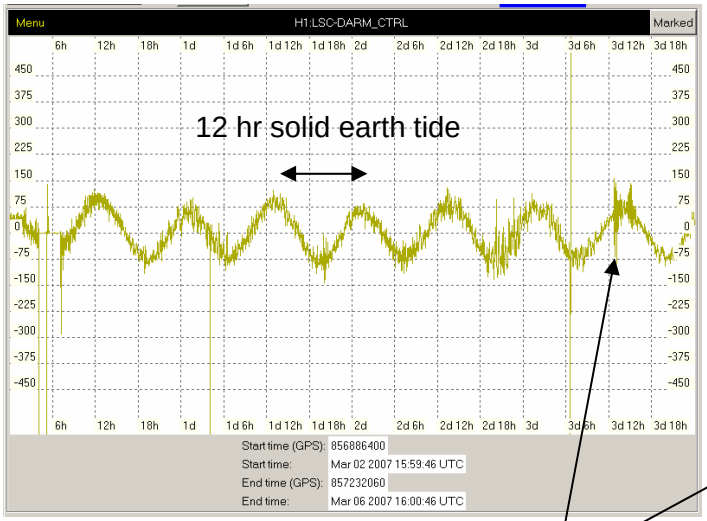

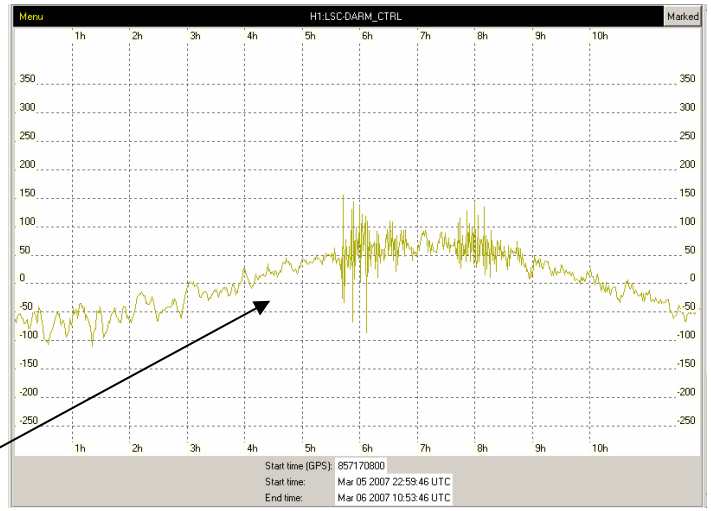

Indonesian Earthquake
2007-March-06
03:49:41 M6.3
05:49:28 M6.1

May be in p-wave shadow zone for viewing from LHO

We see both quakes in DARM_CTRL on a solid earth tide rise as shown in these minute trend plots

Seismic events at Virgo

DATE	Latitude	Longit.	Depth	Richter	DIST	Movement amplitude	Delay of arrival	Delay of maximum	In-Lock duration	Event duration
mo da hh:mm:ss	degree	degree	km	mag.	km	micron	minutes	minutes	minutes	minutes
05 23 04:41:46	52.35	-31.81	10	5.7	3258	25.1	6.9	18	16.2	46
05 30 20:22:12	52.14	157.29	116	6.4	8946	15.4	9.8	23.1	23.2	86.6
06 02 21:34:57	23.03	101.05	5	6.3	8350	31.3	15.3	44.1	43.9	106.6
06 07 00:40:38	-3.32	146.76	4	6.2	13878	12.9	29.9	64.3	74.7	124.6
06 13 19:29:40	13.55	-90.62	23	6.7	9886	71.5	12.9	53.5	24.2	97.8
06 15 18:49:53	1.72	30.83	24	5.9	5095	22.6	15	32.1	25	64.3
06 18 06:18:48	-3.57	150.95	25	6.3	14177	12.8	34.2	64		129.6
06 18 14:29:48	34.44	50.83	5	5.5	3610	10.8	18.3	22.1		24.3
06 24 00:25:18	-55.65	-2.63	10	6.5	11153	17.8	25.5	41.8	55	85.8
06 28 02:52:09	-7.97	154.63	10	6.7	14814	41.9	22.8	68.2	0	128.5
06 29 18:09:11	39.27	20.26	10	5.4	950	65.9	3.1	5.8	4.9	53.8
07 03 08:26:00	0.71	-30.27	10	6.3	6269	58.4	9.9	17.9	17.8	47.4
07 04 01:23:24	55.47	110.30	10	5.3	6718	11.4	35.5	39.1	39.2	40
07 06 01:09:19	16.35	-93.99	113	6.0	9922	6.2	23	23.4		57.9
07 13 21:54:43	51.84	-176.28	35	6.0	9428	6.7	44.6	48.1		50.2
07 15 13:08:00	52.48	-168.05	10	6.1	9375	24.0	23.1	61.8	61.5	81.1
07 16 01:13:22	37.53	138.45	12	6.6	9628	201.9	12.8	56.6	23.4	106.9
07 16 06:37:40	37.50	138.47	15	5.7	9631	11.3	33	56.3		56.9
07 16 14:17:37	36.81	134.85	350	6.8	9505	36.1	12	35	22	99.6
07 17 09:39:27	-26.21	-177.74	10	6.1	18028	11.6	89.2	95		129.8
07 17 14:10:42	-2.73	36.36	8	5.9	5788	14.2	16.6	34.6		37.2
07 17 18:23:21	40.16	21.53	22	5.4	995	7.2	6.7	6.8		19.4
07 18 00:07:35	-26.30	-177.74	10	6.1	18037	12.1	51.8	95.2		113.1
07 21 15:34:52	-22.15	-65.78	289	6.4	10697	10.8	23.2	24		32.2
07 25 23:37:31	7.16	92.52	15	6.1	8860	12.2	22.3	55.1	0	100.8
07 26 05:40:16	2.87	127.46	25	6.9	11962	56.0	18.9	34.4	0	137.5
07 27 14:46:26	-21.46	170.94	10	6.1	17043	10.2	76.5	104.1		109
07 29 04:54:36	53.64	169.70	25	6.0	9066	6.7	48.2	56.3		59.6
07 31 15:07:35	27.34	126.90	10	5.9	9860	24.9	47.2	56.4	52.6	67.5
07 31 22:55:31	-0.16	-17.80	11	6.2	5641	24.8	16.4	16.6	16.9	38.6
08 01 17:08:51	-15.60	167.68	120	7.2	16304	102.2	19.6	73.6	0	110.3
08 02 02:37:42	47.10	141.84	5	6.2	8901	73.3	12.3	51.9	45.3	144.1
08 02 03:21:42	51.30	-179.97	21	6.7	9460	63.0	13	58.7	0	100.1
08 03 00:41:19	-62.91	145.37	41	6.0	16514	4.5	19.8	88		132.8
08 07 00:02:24	27.29	126.84	18	5.9	9860	34.5	14.4	53.4	56.3	75.7
08 08 17:04:56	-5.91	107.70	280	7.5	11092	114.8	13.3	43	13.5	111.5
08 15 20:22:13	50.57	-177.51	21	6.5	9561	31.5	13.2	49.7	49.4	142.7
08 15 23:40:57	-13.41	-76.61	39	8.0	10849	1245.0	13.6	61	14.7	61
08 16 05:16:56	-14.26	-76.08	23	6.3	10872	25.1	26.6	52.8	70.7	81.1
08 16 08:39:28	-9.71	159.38	10	6.7	15269	41.0	40.5	87.4	0	142.5
08 16 11:35:30	-14.39	-76.17	35	6.0	10889	6.0	51.5	53.9	0	55.3
08 16 14:18:24	-3.52	-12.15	10	5.5	5731	6.5	29.2	30.7		57.2
08 17 03:04:03	-5.24	129.50	10	6.4	12778	12.8	11.3	59.5		128.7
08 18 02:52:35	-13.79	-76.26	30	6.0	10850	6.1	26.6	58.3		68.6
08 20 12:37:06	-0.21	-18.16	10	5.7	5664	9.0	16.4	16.6		54.7
08 20 13:46:17	6.16	127.46	8	6.5	11689	17.4	26.1	69.6		85.2
08 20 22:42:29	8.02	-39.27	10	6.5	6251	150.9	9.8	17.7	17.6	91.1
08 25 22:05:49	39.29	41.07	10	5.1	2592	7.5	9.4	13.6		30.7
08 31 20:52:45	36.81	26.14	43	5.2	1532	12.3	7.8	10.5		14.9
09 01 19:14:21	24.82	-109.70	10	6.3	10316	12.7	24.5	56.4		85.4

Maintained lock events

DATE	Latitude	Longit.	Depth	Richter	DIST	Movement amplitude	Delay of arrival	Delay of maximum	Event duration
mo da hh:mm:ss	degree	degree	km	mag.	km	micron	minutes	minutes	minutes
06 18 06:18:48	-3.57	150.95	25	6.3	14177	12.8	34.2	64	129.6
06 18 14:29:48	34.44	50.83	5	5.5	3610	10.8	18.3	22.1	24.3
07 06 01:09:19	16.35	-93.99	113	6.0	9922	6.2	23	23.4	57.9
07 13 21:54:43	51.84	-176.28	35	6.0	9428	6.7	44.6	48.1	50.2
07 16 06:37:40	37.50	138.47	15	5.7	9631	11.3	33	56.3	56.9
07 17 09:39:27	-26.21	-177.74	10	6.1	18028	11.6	89.2	95	129.8
07 17 14:10:42	-2.73	36.36	8	5.9	5788	14.2	16.6	34.6	37.2
07 17 18:23:21	40.16	21.53	22	5.4	995	7.2	6.7	6.8	19.4
07 18 00:07:35	-26.30	-177.74	10	6.1	18037	12.1	51.8	95.2	113.1
07 21 15:34:52	-22.15	-65.78	289	6.4	10697	10.8	23.2	24	32.2
07 27 14:46:26	-21.46	170.94	10	6.1	17043	10.2	76.5	104.1	109
07 29 04:54:36	53.64	169.70	25	6.0	9066	6.7	48.2	56.3	59.6
08 03 00:41:19	-62.91	145.37	41	6.0	16514	4.5	19.8	88	132.8
08 16 14:18:24	-3.52	-12.15	10	5.5	5731	6.5	29.2	30.7	57.2
08 17 03:04:03	-5.24	129.50	10	6.4	12778	12.8	11.3	59.5	128.7
08 18 02:52:35	-13.79	-76.26	30	6.0	10850	6.1	26.6	58.3	68.6
08 20 12:37:06	-0.21	-18.16	10	5.7	5664	9.0	16.4	16.6	54.7
08 20 13:46:17	6.16	127.46	8	6.5	11689	17.4	26.1	69.6	85.2
08 25 22:05:49	39.29	41.07	10	5.1	2592	7.5	9.4	13.6	30.7
08 31 20:52:45	36.81	26.14	43	5.2	1532	12.3	7.8	10.5	14.9
09 01 19:14:21	24.82	-109.70	10	6.3	10316	12.7	24.5	56.4	85.4
09 03 16:14:53	45.79	150.05	96	6.3	9350	20.4	22.5	46	91.7
09 05 05:08:16	41.36	19.48	10	4.8	782	7.6	5	5	6.8
09 06 17:51:26	24.35	122.28	50	6.5	9803	15.3	12.8	56.1	101.9
09 05 05:08:16	41.36	19.48	10	4.8	782	7.6	5	5	6.8

LIGO

Locked and partially locked events

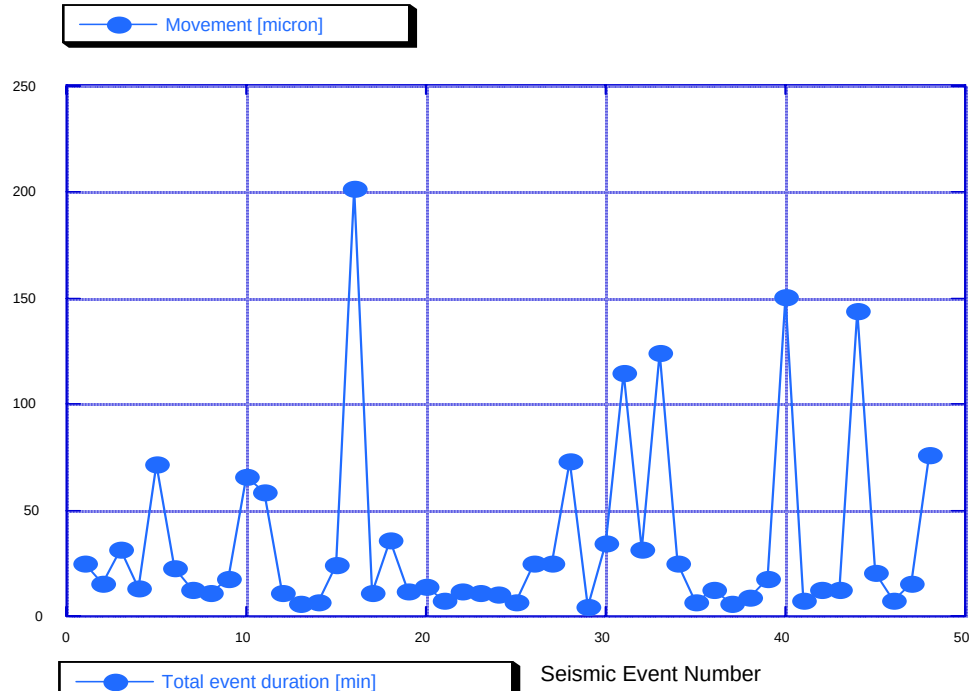

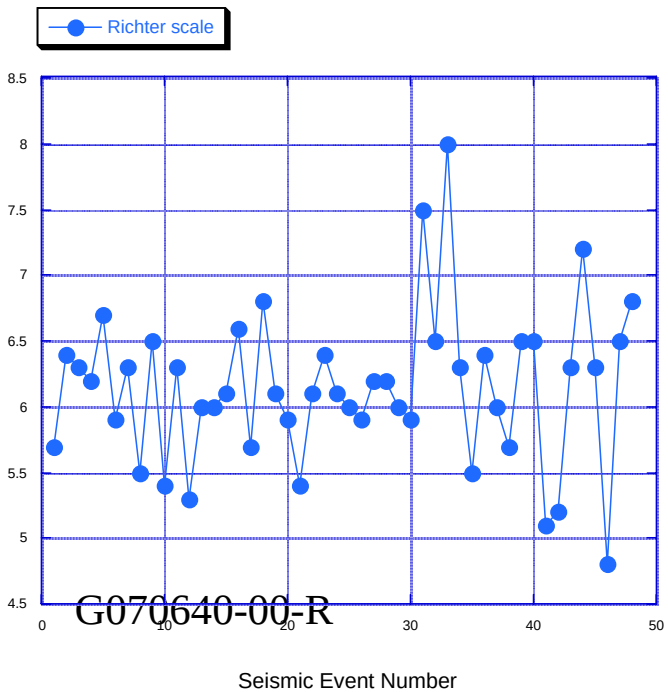

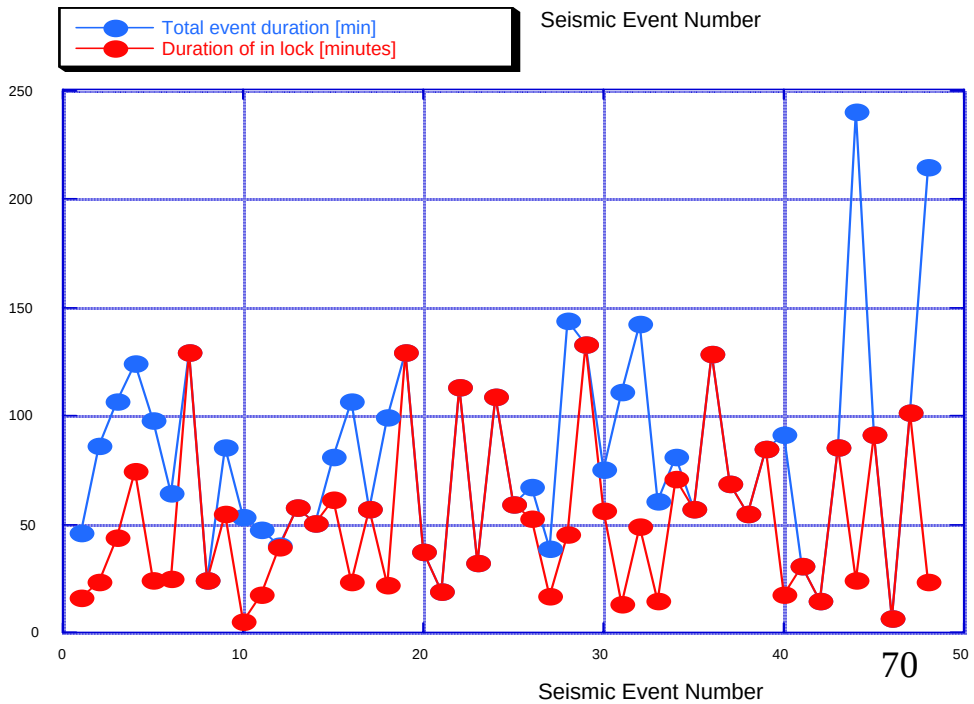

Fully locked events

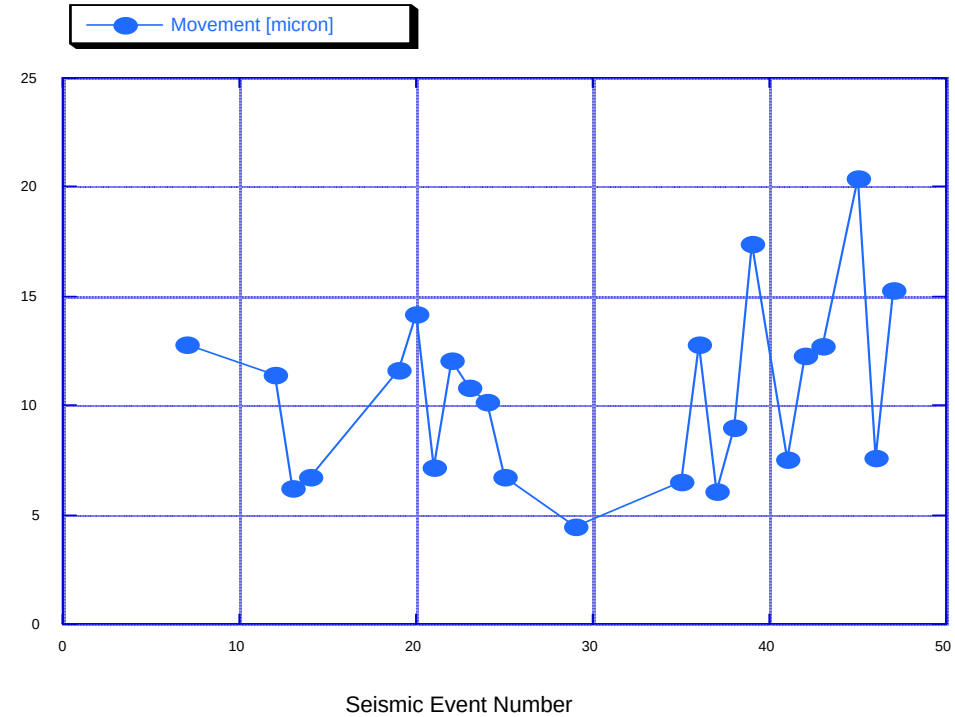

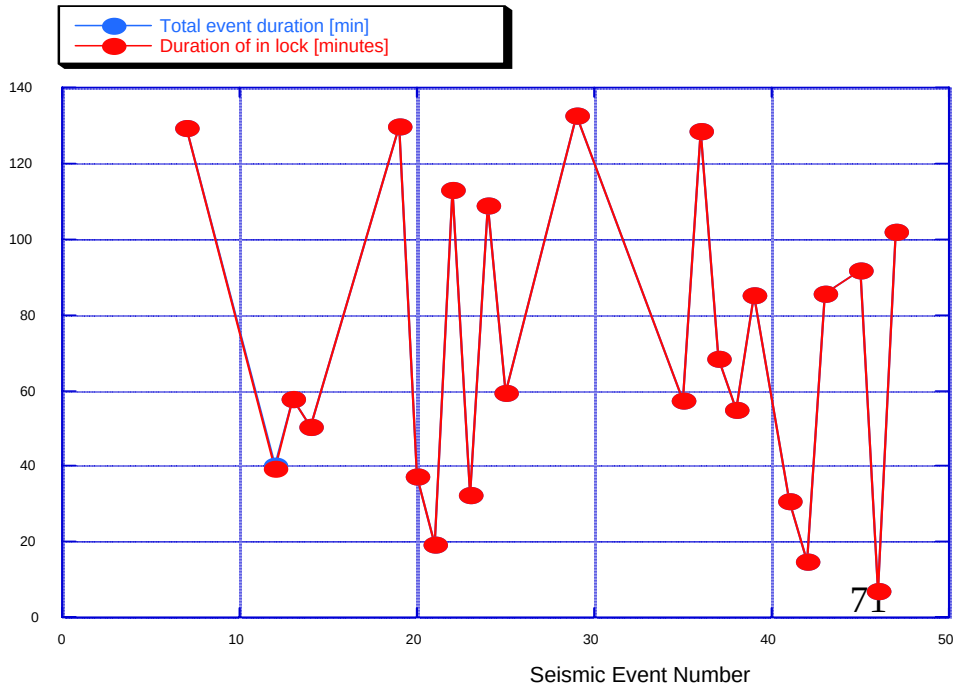

LIGO

Full interferometer signal

- The transfer function can be bypassed with proper optical links to ground
- Presently no interest to do so by GW scientists
- Could do if sufficient interest was shown

- Next generation of GW interferometers deep underground
- Sensitive to Earth's modes

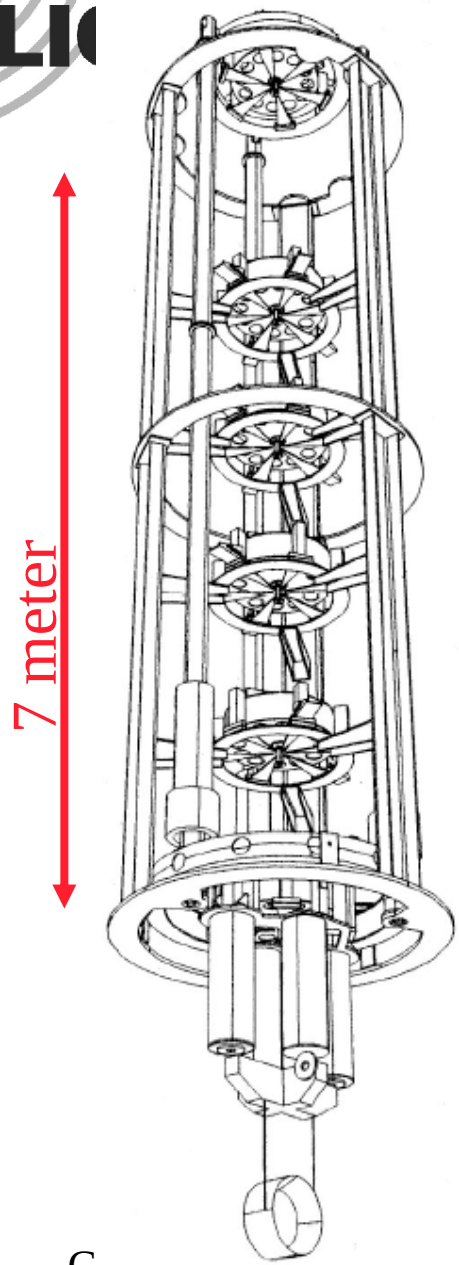

Seismic isolators as seismometers

- The seismic attenuators IP and attenuation filters are the largest and probably the most sensitive seismometers in the world

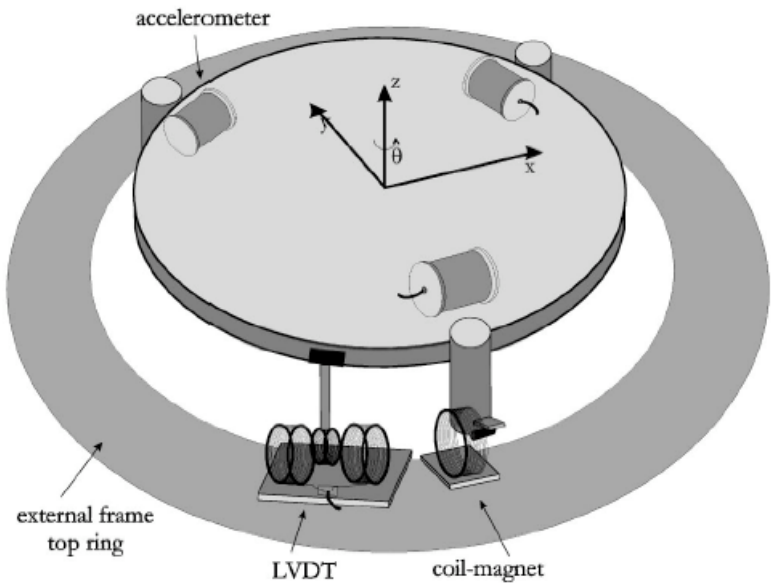

Inertial bench sensors give full 6 d.o.f. readout

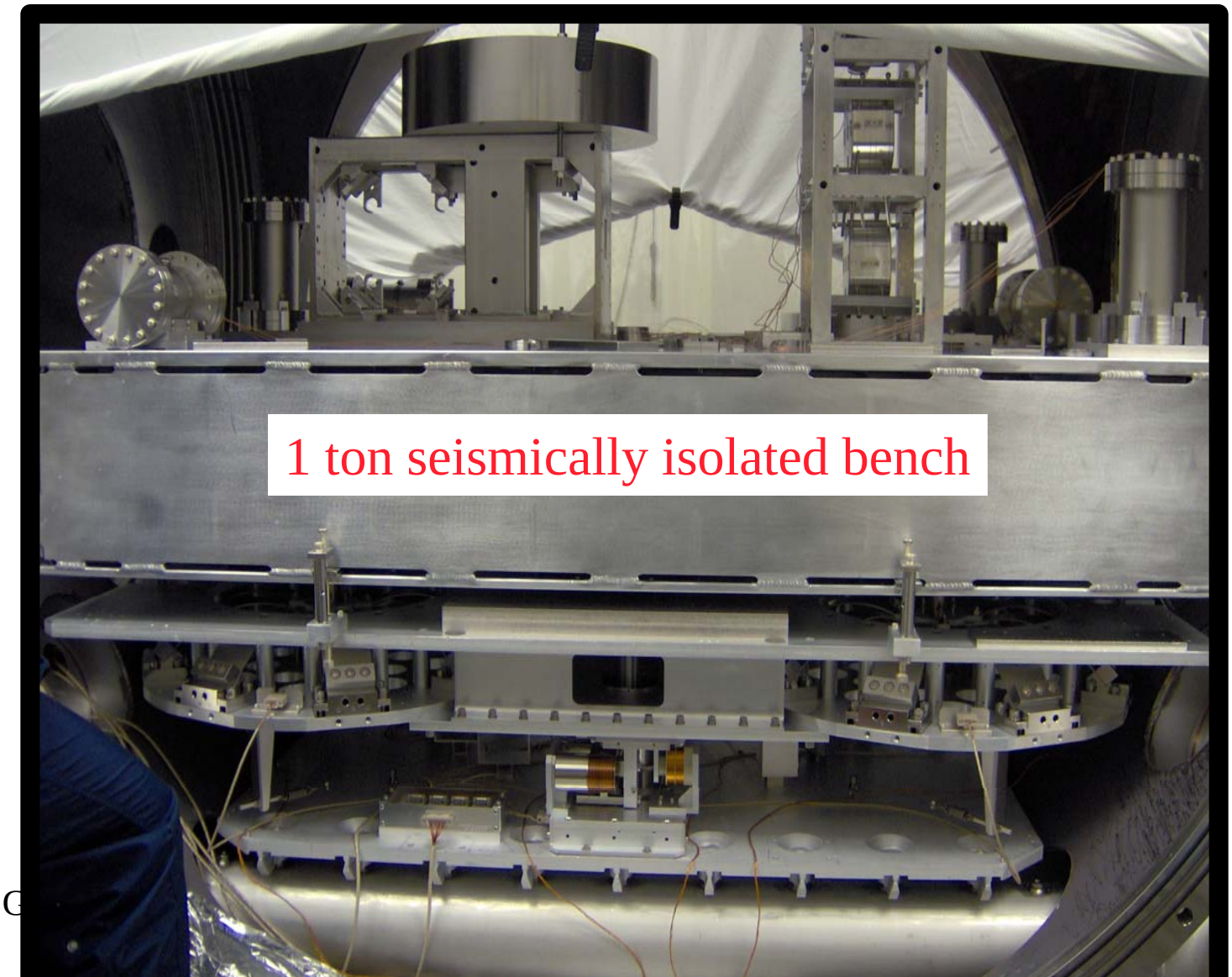

LIGO

- GW optical benches can be a great
  - Seismically isolated
  - Actuatable
  - Testing platform